The analytical representation of electronic potential-energy surfaces

George C. Schatz

Department of Chemistry, Northwestern University, Evanston, Illinois 60208

This article reviews the commonly used methods for representing electronic potential-energy surfaces for small molecules and simple chemical reactions in terms of globally defined analytical functions. Four classes of methods are discussed: spline fitting methods, semiempirical methods, many-body expansion methods, and methods that represent global surfaces based on information determined along reaction paths. The application of these methods is examined in detail for four triatomic systems and one four-atom system: $O(^3P)+H_2$, $Cl+HCl$, $H+CO$, $O(^1D)+H_2\rightarrow H_2O\rightarrow OH+H$, and $H+CO_2\rightarrow OH+CO$. These examples illustrate both the art and the pitfalls of representing surfaces. In addition, the consequences of different potential surface representations for the dynamics of collisions on these surfaces are discussed at length.

CONTENTS

I. Introduction 669
II. Methods for Fitting Surfaces 671
A. Spline fitting methods 671
B. Semiempirical and related methods 673
C. Fits based on many-body expansions 674
D. Global surfaces based on reaction paths 675
III. Case Studies of Selected Triatomic Surfaces 676
A. $O+H_2$ 676
B. $Cl+HCl$ 678
C. $H+CO$ 680
D. H_2O $[O(^1D)+H_2\rightarrow OH(^2\Pi)+H]$ 682
IV. Potential-Energy Surfaces for $n>3$ Polyatomic Molecules: $H+CO_2$ 684
V. Conclusions 686
Acknowledgments 687
References 687

I. INTRODUCTION

A major problem in the use of electronic potential energies derived from quantum-electronic structure ("*ab initio*") calculations as a basis for spectroscopic and dynamics studies is the development of realistic global representations of these potential-energy surfaces. Although this problem has rarely been given the attention it deserves in the scientific literature, it continues to grow in importance as experiments provide increasingly more sophisticated probes of molecules and reactions involving three or more atoms, and as *ab initio* methods become increasingly capable of determining accurate energies for these molecules and reactions. In this paper I should like to address the issue of how to represent the potential surfaces that arise in studies of unimolecular decay of highly excited molecules and in bimolecular reactions dynamics, with an emphasis on what strategies are available, what are their virtues and weaknesses, and what systems they have been used on. To make the review tractable, I have chosen to restrict the types of potential surfaces considered to those that describe bond breaking or forming in gas-phase bimolecular and unimolecular reactions, with special emphasis on atom addition and atom transfer reactions. In many respects this class of potential surface is the most difficult to represent, as it involves the *global* behavior of the potential-energy function, and this function depends on many $(3n-6)$ internal coordinates (where n is the number of atoms). Since global surfaces are desired, the very powerful polynomial (actually multinomial) expansion methods that are so often used for representing local regions of potentials (say, for describing molecular vibrational motions) are not applicable. An additional complication associated with potential functions that describe bond breaking and bond formation is that the functional dependence cannot usually be represented using multipole expansions, or in terms of the additive contributions of single-variable functions such as pair potentials. This contrasts with the situation for surfaces that are commonly used in describing van der Waals forces, hydrogen bonding, and other electrostatic interactions. The latter types of potentials have been well studied in molecular modeling applications, and accurate empirical potential surfaces have been developed using relatively simple functions (see, for example, Kollman, 1987; Stone and Price, 1988). Such potentials may be useful for describing the nonreactive "part" of the potential surfaces that are considered here, but this aspect will not be emphasized. It is also important to note that a number of electronic structure models that are useful for describing large many-body clusters and solids are not sufficiently accurate for the small covalently bonded molecular systems that we consider here. These include the embedded-atom method (Daw and Baskes, 1984) and the related effective-medium method (Jacobson *et al.*, 1987; Kress and DePristo, 1988, and references therein).

The need for developing analytical representations of the potential-energy surfaces that are determined from *ab initio* calculations arises because these calculations are sufficiently time consuming that the explicit calculation of energies and energy gradients at every point needed in a dynamics study is rarely feasible. In addition, *ab initio* calculations usually do not provide potential energies that are accurate enough to be used without at least some adjustment, and the development of analytical representations facilitates this adjustment. Analytical representations can also be useful for the visualization of potential surface features, for the characterization of topological

features that may not be evident from a coarse-grained *ab initio* study (particularly for reactions of high dimensionality), and to provide "building blocks" by which surfaces for molecules too complex to be studied by *ab initio* methods can be constructed.

All of these comments about the usefulness of analytical representations of potential surfaces are, however, irrelevant if the representation is qualitatively inaccurate or is otherwise defective. Unfortunately the only global surface developed to date for a triatomic or larger system that is known to "chemical accuracy" (i.e., to within roughly 0.05 eV) is that for the $H+H_2$ reaction (see Varandas *et al.*, 1987). Accurate dynamics studies using this and an earlier surface (reviewed by Schatz, 1988b) have produced a large number of results in excellent agreement with experiment. In addition, a number of dynamical results have been predicted by theory that stimulated subsequent successful experiments. This indicates the types of rewards that are possible with an accurate surface, but, as we shall see, compromises are necessary when one considers systems more complicated than $H+H_2$.

Wright and Gray (1978) have presented a list of criteria that a successful representation of a potential surface must satisfy. Their list is based on an earlier one by Kuntz (1976), and related discussions have been given elsewhere (Sathymurthy and Raff, 1975; Gittens *et al.*, 1977; Connor, 1979). The Wright and Gray criteria for an analytical representation are as follows.

(1) It should accurately characterize the asymptotic reactant and product molecules (or more generally any fragment of the full system).

(2) It should have the correct symmetry properties of the system.

(3) It should represent the true potential accurately in interaction regions for which experimental or nonempirical theoretical data are available.

(4) It should behave in a physically reasonable manner in those parts of the interaction region for which no experimental or theoretical data are available.

(5) It should smoothly connect the asymptotic and interaction region in a physically reasonable way.

(6) The interpolating function and its derivatives should have as simple an algebraic form as possible consistent with the desired goodness of fit.

(7) It should require as small a number of data points as possible to achieve an accurate fit.

(8) It should converge to the true surface as more data become available.

(9) It should indicate where it is most meaningful to compute the data points.

(10) It should have a minimal amount of *ad hoc* or "patched up" character.

As discussed by Connor (1979), criteria (1)–(5) are essential if the representation is to be useful for dynamics calculations, while criteria (6)–(10) are less essential though highly desirable. Note that some of the criteria lead to conflicting strategies for developing fits. For example, in order to satisfy criterion (4) that surfaces be globally acceptable for all possible arrangements of the atoms, it may be necessary to use complex functions that violate criterion (6). Moreover, it is often easiest to enforce identical atom symmetry [criterion (2)] by permuting atom coordinates in the potential function, but this may lead to a surface that is not smooth [violating criterion (5)] for certain geometries.

Because of the complexity of satisfying the Wright and Gray criteria, and the different computational capabilities and interests of the researchers who have tackled the problem of representing surfaces, a number of rather different methods have been developed and are still in common use for representing surfaces. Section II of this review will be concerned with describing these methods, and for this purpose we shall subdivide them into four groups: (a) spline fitting methods, (b) methods in which semiempirical potential surfaces are either fitted or corrected in order to match *ab initio* calculations or experiment, (c) empirical fits based on many-body expansions, and (d) global surfaces that are defined using information determined along a reaction path. It should be emphasized that these groupings are not unique, and many surfaces have been developed using combinations of two or more groups of methods.

Note that we shall not consider fitting functions that define global molecular surfaces that do not dissociate correctly, nor shall we consider fitting functions that produce "effective" potential surfaces that do not explicitly include all degrees of freedom. Both types of surfaces have commonly been developed in fits to spectroscopic data where only locally defined information about the potential surface is available. An example of a fitting function that does not, in general, dissociate correctly is the Simons-Parr-Finlan (SPF) function (Simons *et al.*, 1973; Simons, 1974). This expands the surface in a multinomial in the variable $S=(R-R_e)/R$ for each internuclear coordinate R, with R_e being the equilibrium value of R. Since $S\rightarrow 1$ for large R, the SPF function dissociates to a constant function of R, but the dissociation energy is not, in general, correct unless global information is used in developing the fit, and this is rarely done. In addition, SPF functions do not generally describe the dissociated fragment potentials correctly. Other fitting functions that are similarly restricted exist, and to illustrate the limitations of these "global-like" functions, we shall describe one commonly used H_2O surface that falls into this category in Sec. III.D. Global-like or effective potential surfaces are often used in molecular dynamics simulations, since they can be chosen to be simple functions such as sums of pair potentials, but are still quite accurate in describing molecular properties near equilibrium.

All four of the fitting methods that we consider have been used rather extensively to describe *triatomic* potential surfaces, and several of these surfaces will be described in Sec. III. Rather than reviewing all the triatomic surfaces that have been developed, we shall focus on four systems for which independent surfaces have

been developed using two or more of these methods: $O+H_2 \rightarrow OH+H$, $Cl+HCl \rightarrow ClH+Cl$, $H+CO \rightarrow HCO$, and H_2O [i.e., $O(^1D)+H_2 \rightarrow OH+H$]. All of these examples represent systems for which the surfaces are known at a level beyond simple empirical fits, but not yet known within chemical accuracy. In addition, these four systems have all been extensively studied using dynamics calculations, so we shall be able to examine not only the process of representing surfaces but also the dynamical picture of the reaction that arises from each representation. This dynamical picture is sometimes strongly dependent on potential surface. Finally, the molecular systems that we shall consider have generally been the subject of extensive dynamics and spectroscopic experiments, so tests of the adequacy of the surfaces have generally been performed.

For reactions involving four atoms or more ($n > 3$), the technology of representing potential surfaces is in a much more primitive state, and only a few global potential surfaces that describe bond breakage and formation have been developed, most of which are highly empirical. Section IV will focus on the $n > 3$ surfaces, with an extensive discussion of the surface for $H+CO_2 \rightarrow OH+CO$. Included in this section will be detailed accounts of fitting strategies, pitfalls, and dynamical results.

One point that is not addressed by the Wright and Gray criteria is the issue of multiple potential surfaces. Although many chemical processes may be described accurately using a single electronically adiabatic potential surface, the formation and breaking of bonds very often involves several surfaces, and it is important to allow for them in some sense. Ideally one should develop analytical representations of all energetically relevant potential surfaces and their couplings, taking care to describe interactions between surfaces in a mathematically consistent way (i.e., using a single double-valued function to describe two surfaces that have a conical intersection). This ideal has rarely been achieved. ($H+H_2$ is one of the exceptions. See Varandas *et al.*, 1987.) More often, the many-coupled-surface problem has been approximated using either uncoupled surfaces or just a single surface. Although the general topic of multiple potential surfaces is beyond the scope of this review, we will discuss specific features of this problem in our examples in Secs. III and IV.

There have been several reviews in the past of methods for representing gas-phase potential surfaces, and the one that most closely overlaps with the present review is that by Truhlar *et al.* (1987), which considers the literature through 1986. This comprehensive review emphasized larger polyatomic systems more than we shall and included a major section on calculating reaction paths using *ab initio* methods. The present review will emphasize the methodology of representing surfaces more than they did, with extensive discussion of the four triatomic reactions mentioned above that have been studied using more than one surface fitting method. In addition, we shall highlight several surfaces that were not considered by Truhlar *et al.*, and we shall describe the interaction between surface fitting and dynamics calculations in much more detail.

Other reviews of methods for representing potential surfaces include the books by Hirst (1985) and Murrell *et al.* (1984) and the articles by Sathyamurthy (1985) and Connor (1979). Hirst's book includes a general discussion of potential surface determination, with an emphasis on *ab initio* methods (and in this regard, see, also, the review by Dunning and Harding, 1985), but it only briefly describes methods for representing potential surfaces. The book by Murrell *et al.* emphasizes the many-body expansion method for representing potential surfaces, which we describe in Sec. II.D. Our discussion will update the many uses of this method. Sathyamurthy's review is broader based than the present one in that nonreactive surfaces are considered, while Connor's review also includes extensive material on dynamics calculations. One topic that we shall discuss only briefly is the methodology underlying semiempirical electronic structure calculations. A review of these methods is given by Kuntz (1985).

II. METHODS FOR FITTING SURFACES

A. Spline fitting methods

If the cost of calculating *ab initio* energies is not too high, then the most straightforward approach to fitting a surface is to use interpolation. Spline interpolation in particular provides a very flexible and numerically efficient approach for doing this that gives a surface with smooth first and continuous second derivatives (needed for trajectory integration, reaction path, and force-constant analysis). Since spline methods require a fairly high density of points to generate surfaces that are free from artifacts, they have mainly been used to determine surfaces that depend on one, two, or at most three variables, and as a result their primary area of application has been to triatomic molecular potential surfaces.

The first use of spline methods to fit *ab initio* calculations depending on two or three coordinates was by McLaughlin and Thompson (1973) and by Sathyamurthy and co-workers (1975, 1976), who developed surfaces for $HeH^+ + H_2$, $He+H_2^+$, and $D+HCl$. More recently, Bowman, Bittman, and Harding (BBH; 1985) have developed a three-dimensional spline representation of the HCO potential surface, and this will be described in detail in Sec. III.C. The BBH surface is not simply a fit to *ab initio* energies. Instead, 2000 *ab initio* points were first fitted to locally defined polynomials based on Simons-Parr-Finlan functions (Simons *et al.*, 1973; Simons, 1974). The locally defined functions were then smoothly combined using hyperbolic tangent-switching functions; adjustments to HCO minima and dissociation saddle points were made to match experiment, and the resulting global surface was evaluated at 40 000 points to define a grid for the three-dimensional spline calculation.

The resulting fit involved 250 000 spline coefficients, but despite this large number, the computer time needed for the evaluation of the spline function was only five times longer (Geiger *et al.*, 1985) than that needed for a much simpler many-body surface. One defect of the BBH surface is that it does not describe dissociation of HCO into C+OH or O+CH.

Although two- and three-dimensional global spline surfaces have been developed for other systems than those described above (Chapman *et al.*, 1983), the need for large numbers of *ab initio* calculations has limited the usefulness of this approach. An alternative method that is more efficient in this regard for some types of potential surfaces is the rotated Morse spline (RMS) method. This method was originally developed by Bowman and Kuppermann (1975; see also Gray and Wright, 1977), and it was designed to describe surfaces with a single reaction path in which one bond forms while the other breaks. Figure 1 shows a schematic of the coordinates involved for the system $A+BC\rightarrow AB+C$ using the coordinates r_{AB} and r_{BC}. The solid curve indicates a possible reaction path between the $A+BC$ region (labeled I), through the region of strong three-body interaction (labeled III) into the $C+AB$ region (labeled II). Region IV locates geometries in which all three atoms are substantially separated, corresponding to dissociation.

The RMS method is based on the fact that, for many reactions, one can define a "swing point" r^*_{AB}, r^*_{BC} in Fig. 1 such that the potential in region II can be represented by a Morse function that is rotated about this point. Defining the angle φ as indicated in Fig. 1, then the potential in region III is

$$V(r_{AB},r_{BC}) = D(\varphi)[(1-\exp\{\beta(\varphi)[l-l_e(\varphi)]\})^2-1]+D_{BC}\ , \tag{1}$$

where

$$l=[(r^*_{AB}-r_{AB})^2+(r^*_{BC}-r_{BC})^2]^{1/2}\ , \tag{2}$$

$$\varphi=\tan^{-1}\left[\frac{r^*_{BC}-r_{BC}}{r^*_{AB}-r_{AB}}\right]\ . \tag{3}$$

The Morse parameters $D(\varphi)$, $\beta(\varphi)$, and $l_e(\varphi)$ are functions of φ which are best determined (Schatz *et al.*, 1981) by one-dimensional spline fits to Morse parameters that are determined by least-squares fits to *ab initio* points at selected fixed φ cuts. In this case φ varies from 0 to 90°.

To complete the specification of the potential it is necessary to define the potential in regions I and II. Often the potential at $\varphi=0$ is not equal to its $r_{AB}\rightarrow\infty$ asymptotic form, and likewise that at $\varphi=90$ is not equal to that at $r_{BC}\rightarrow\infty$, so some sort of interpolation is needed. A common prescription (Schatz *et al.*, 1981; Garrett *et al.*, 1983) involves using an exponential to interpolate Morse functions between the asymptotic and $\varphi=0$ or $\varphi=90°$ limits. For example, in region I we would write

$$V(r_{AB},r_{BC}) = D(r_{BC})(1-\exp\{-\beta(r_{BC})[r_{AB}-r_e(r_{BC})]\})^2 + D_{BC}\ , \tag{4}$$

where

$$D(r_{BC})=D_{BC}-[D_{BC}-D(0°)]\exp[-\alpha(r_{AB}-r^*_{AB})]\ , \tag{5}$$

$$\beta(r_{BC})=\beta_{BC}-[\beta_{BC}-\beta(0°)]\exp[-\alpha(r_{AB}-r^*_{AB})]\ , \tag{6}$$

$$r_e(r_{BC})=r_{eBC}-[l^*_{BC}-l_e(0°)]\exp[-\alpha(r_{AB}-r^*_{AB})]\ . \tag{7}$$

Note that $l^*_{BC}=r^*_{BC}-r_{eBC}$ and D_{BC}, β_{BC}, r_{eBC} are the isolated BC Morse parameters.

The parameter α determines the rate at which the switch between asymptotic and $\varphi=0°$ limits occurs, and one way to determine it that does not require additional information beyond what is needed to fit region III is to require that the derivative of the potential with respect to φ be smooth at $\varphi=0°$ (at the junction of regions I and III). Unfortunately this match between Cartesian and polar coordinate regions is imperfect for two reasons. First, the match between the derivatives can be made exact at only one value of l, so there will be a discontinuity in the derivatives of the potential that could make it difficult to integrate trajectories. Second, the determination of α by forcing continuity of the derivatives rarely defines an asymptotic potential that is accurate, since the "tail" of the potential is not usually a simple exponential.

One way to avoid the derivative discontinuity problem

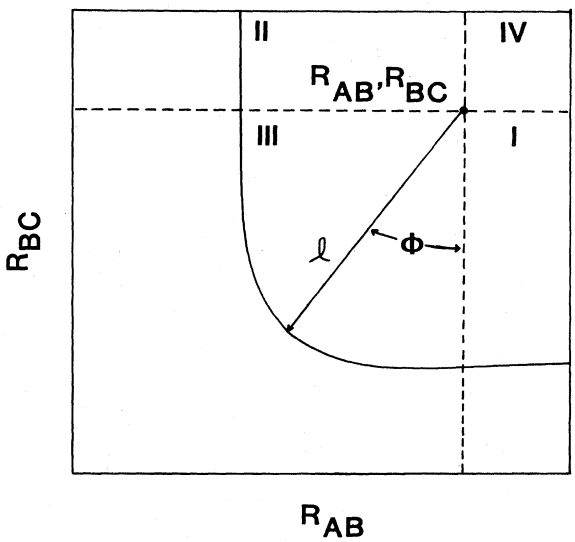

FIG. 1. Coordinates l and φ used in defining rotated Morse spline representation of potential surface for a three-atom (ABC) surface using the R_{AB} and R_{BC} internuclear distances. R^*_{AB} and R^*_{BC} are the swing-point coordinates. Dashed lines divide configuration space into four regions I, II, III, and IV that are defined in the text.

that is similar to a procedure recently used by Joseph *et al.* (1988) is to define the swing point so that the potential is asymptotic at $\varphi=0°$ and $\varphi=90°$. In this case the derivatives of the D, β, and r_e parameters with respect to φ can be forced to be zero at the boundaries, no interpolation is needed in regions I and II, and the potential is automatically smooth. A defect of this procedure is that the swing-point location needed to ensure that the potential is asymptotic at $\varphi=0°$ and 90° may not be very efficient for representing the potential in region III. What Joseph *et al.* actually did was to use a swing-point location that was efficient in region III, and force the Morse parameters to become asymptotic at shorter range than they should be. An improvement to this procedure which has not been considered would be to add in additional functions to the Joseph *et al.* potential that describe the "tail" regions. These functions would be functions of internuclear or Jacobi coordinates that would overlap regions I and III or regions II and III, but they would vanish in region III where the RMS fit is accurate.

The RMS procedure has now been used to fit a number of surfaces, including the $O(^3P)+H_2$ and Cl+HCl surfaces that will be discussed in Sec. III (Schatz *et al.*, 1981; Garrett *et al.*, 1983; Joseph *et al.*, 1988). A general discussion of how best to select cuts for doing *ab initio* calculations has been presented by Wagner *et al.*, (1981), and this has led to fits for $O(^3P)+H_2$ (Schatz *et al.*, 1981) and Cl+HCl (Garrett *et al.*, 1983) in which the fitting and *ab initio* calculations were done interactively. This greatly reduces the number of *ab initio* points needed [33 for $O(^3P)+H_2$, 18 for Cl+HCl].

The RMS surfaces described so far have all been functions of two mathematical dimensions (r_{AB}, r_{BC}), but in general one needs functions of three dimensions for a triatomic (and more for higher polyatomics). An obvious extension of the RMS method to more dimensions is to let the D, β, and l_e parameters be functions of additional coordinates and use multidimensional spline functions to represent this dependence. However, a major flaw with this scheme is that the rotated Morse representation of a surface is inappropriate for describing that surface at least somewhere in configuration space if that surface has more than one reaction path (i.e., more than two asymptotic arrangement channels). Since this situation is *very* common, the extension of RMS to additional dimensions has typically been done only in a local sense (Garrett *et al.*, 1983; Bowman *et al.*, 1984), such as via quadratic (or other low-order) multinomial expansions in the degrees of freedom not explicitly involved in bond formation and breaking.

Joseph *et al.* (1988) have recently presented one approach for generating global surfaces from the RMS method for a reaction involving three reaction paths. For $O(^3P)+H_2$ they first developed local fits for the two equivalent $O+H_2\rightarrow OH+H$ rearrangement paths by using RMS for the collinear surface and a quadratic-quartic treatment of the bend. They then developed a global surface by switching between the two local surfaces, using a switching variable that is very close to the orientation angle between the O—H_2 and H—H Jacobi vectors. By adjusting the functional form of the switching function, they were able to adjust the saddle point for the third rearrangement path ($H+OH\rightarrow HO+H$) to a reasonable value compared to *ab initio* calculations. It is not clear from their analysis, however, whether this rearrangement path is globally defined away from the saddle point.

B. Semiempirical and related methods

The idea behind these methods is to use a relatively simple molecular-orbital theory to define the potential surface of interest in such a way that it can be adjusted to match *ab initio* calculations or experiment. The adjustments are usually made either by varying parameters that arise naturally in the semiempirical calculations or by adding locally defined correction functions to the semiempirical surface in order to "fix up" special regions of the potential surface such as barriers or minima.

Because *ab initio* methods rarely determine potential surfaces to chemical accuracy, semiempirical methods are very popular, as they provide a relatively simple way to adjust local regions of the potential while retaining the correct global behavior. However, a major defect of semiempirical methods is that the molecular-orbital method used may be so seriously in error that simple adjustments are not sufficient to make the surface accurate.

The most commonly used semiempirical potential function for triatomic reactions that have a single barrier between the reagents and products, and no three-atom wells, is the LEPS (London-Eyring-Polanyi-Sato) surface (Sato, 1955a, 1955b, 1955c). This surface may be considered to be a particular parametrization of the lowest eigenvalue that is derived from an application of the diatomics-in-molecules (DIM) semiempirical molecular-orbital method (Ellison, 1963; Tully, 1977; Kuntz, 1979) to three atoms that have only *s*-type orbitals. LEPS is often used, however, to describe surfaces for atoms with *p*-type orbitals, but in this case one should consider LEPS as just a fitting function rather than a true semiempirical method. Commonly the LEPS function is used in its extended form (Kuntz *et al.*, 1966), where it contains three adjustable constants (Sato parameters) that can be chosen to fit certain properties of the surface, such as saddle-point energy, location, vibrational frequencies, etc. However, the LEPS function is relatively inflexible in that saddle points are invariably found for linear configurations of the three atoms. In addition, a choice of the Sato parameters that optimizes the saddle point for one reaction path (say $F+H_2\rightarrow HF+H$) may do poorly for another path in the same system ($H+FH\rightarrow HF+H$). (See Bender *et al.*, 1975; Botschwina and Meyer, 1977; Wadt and Winter, 1977.) Thus, although the LEPS function has been widely used (as reviewed by Connor, 1979, and Truhlar *et al.*, 1987), it is prudent to be critical of apparent success in applications. This will be rather

dramatically demonstrated in Sec. III.B in our discussion of Cl+HCl.

In recent years a number of approaches have been suggested for improving and generalizing the LEPS function. The very successful LSTH surface (Liu, 1973; Siegbahn and Liu, 1978; Truhlar and Horowitz, 1978) for $H+H_2$ is based on summing a London (i.e., LEPS-like) function with empirically determined short-range functions to fit *ab initio* calculations. This form was retained in the more recent double-many-body-expansion surface (Varandas *et al.*, 1977) that also describes the first electronically excited H_3 surface. A second generalization of LEPS that has been used for the $F+H_2$ surface involves letting the Sato parameters be functions of the triatomic internal coordinates (Brown *et al.*, 1985; Steckler *et al.*, 1985; Takayanagi and Sato, 1988). Usually a simple functional dependence is assumed (such as a low-order cosine Fourier expansion in terms of the bend angle) and the coefficients are adjusted to optimize desired properties. Major advantages of this approach are that it allows barriers to be at nonlinear geometries, and multiple saddle points on the same surface can be separately optimized. A third generalization of LEPS is to seek out alternative parametrizations of DIM that still have the simplicity of LEPS (see Viswanathan *et al.*, 1985). Last and Baer (1981) and Baer and Last (1981) have added a three-center term to the DIM treatment of three *s* orbitals, leading to the LEP-3*C* function, which more realistically describes electronic interactions for $H+XH \rightarrow HX+H$ (X=halogen) reactions. They have also developed a similar surface that allows for *p* orbitals (the DIM-3*C* surface), but this surface and other "complete" DIM surfaces (Stine and Muckerman, 1976) are more complicated functions in which matrices larger than 2×2 must be diagonalized for every surface evaluation.

DIM has also been used to develop surfaces for reactions involving four or more atoms (Eaker and Parr, 1976), with the most extensive applications being to the $H_2^+ + H_2$ reaction (Pederson and Porter, 1967; Krenos *et al.*, 1976; Polak, 1976; Stine and Muckerman, 1978). The H_4^+ surface requires the diagonalization of an 8×8 matrix at every geometry, which makes dynamics studies using trajectories quite tedious, though still feasible. $H_2^+ + H_2 \rightarrow H_3^+ + H$ is a reaction in which several potential surfaces are actively involved, but DIM describes them all reasonably well. These DIM surfaces are especially useful in dynamics studies, since the coupling between surfaces is also available with little additional effort beyond that needed to determine the surfaces. Unfortunately, the "complete" application of DIM to $n>3$ atom reactions is for the most part computationally impractical and subject to serious errors. As a result, the most common use of semiempirical methods for >3 atom reactions has been to construct the potentials associated with three atom fragments, which are then combined using many-body expansions.

C. Fits based on many-body expansions

A very general approach to the representation of potential surfaces involves a many-body expansion of the type

$$V=\sum_{i<j} V_2(r_{ij})+\sum_{i<j<k} V_3(r_{ij},r_{ik},r_{jk})+\cdots, \tag{8}$$

where r_{ij} is the distance between atoms i and j, so that $V_2(r_{ij})$ represents the two-body interaction associated with the ij pair in the absence of the other atoms. Similarly, V_3 is the three-body interaction associated with the ijk cluster (i.e., the total ijk energy minus the sum of two-body energies). Expansions similar to Eq. (8) are at the heart of representations of nonreactive surfaces where van der Waals and hydrogen bond interactions are dominant. For this type of surface, the two-body part of the expansion is very often substantially larger than the higher terms, so that a surface that includes only two-body terms is already useful for dynamics calculations.

For reactive surfaces involving small molecular systems (three to five atoms), Eq. (8) is usually not rapidly convergent at geometries where all the atoms are close together, but this form for representing the potential can still be useful for a number of reasons. One rather obvious reason is that if Eq. (8) is used to represent an n-atom system, and if all the terms up through $n-1$ are accurately determined, then the resulting surface will dissociate correctly into any possible fragment no matter how poorly the nth term is described. This is in contrast to DIM surfaces, where only diatomic and atomic fragments are described correctly. A second reason is that all n-body terms in Eq. (8) are necessarily of finite range and thus can be represented in terms of simpler functions than are needed for global infinite-range representations such as DIM.

The most extensive work on using many-body expansions for small molecule surfaces has been that of Murrell and co-workers (see Murrell *et al.*, 1984). In many of their surfaces (though not all), the two-body potentials have been represented by the extended Rydberg formula,

$$V_2(r)=-D_e\left[1+\sum_k a_k(r-r_e)^k\right]\exp[-\gamma(r-r_e)], \tag{9}$$

and the three-body and higher-order terms have been expressed as products of multinomials and switching functions, as in

$$V_3(r_a,r_b,r_c)=\prod_i (\tfrac{1}{2})[1-\tanh\gamma_i(r_i-r_i')]\left[b_0+\sum_i b_i(r_i-r_i')+\sum_{i<j} b_{ij}(r_i-r_i')(r_j-r_j')+\cdots\right], \tag{10}$$

where r_i $(i=a,b,c)$ defines an internuclear distance or some other internal coordinate. In Eq. (10) the parameters γ_i and distances r_i' are chosen so that the multinomial represents the short-range part of the potential accurately but is turned off by the hyperbolic function at longer range ($r_i \gg r_i'$), where only the two-body potentials are needed. The multinomial coefficients b_i, b_{ij}, etc., are determined by fitting either experimentally derived force fields or *ab initio* data. Since V_3 depends linearly on these coefficients, they may be determined by linear least-squares or by algebraic interpolation techniques (Redmon and Schatz, 1981).

In contrast to the DIM-based semiempirical methods, the number of nonlinear parameters that must be optimized is relatively few, so using Eqs. (8)–(10) to fit surfaces is relatively simple, and as a result this fitting method has been quite extensively used, as is documented in Murrell *et al.* (1984). There are, however, certain points of ambiguity or additional complexity that constitute drawbacks to using this method. One is that although Eqs. (8)–(10) can readily represent surfaces in any dissociative fragment region and in any n-atom local region, the transition region between local and dissociative regions may not be described correctly. This is because Eq. (10) is only a mathematically convenient expression that does not contain any physical content, so it is possible that fits to anything less than global data may have spurious features (extra minima, incorrect correlations in the interactions between different coordinates, etc.). We shall present examples in Secs. III.C and III.D that illustrate this. A second problem is that it is often difficult to use the polynomial representation in Eq. (10) to describe more than one n-atom stationary point (such as two minima separated by a saddle point). One can, of course, superimpose several functions such as Eq. (10) that are expanded about different locations, but this adds considerably to the complexity of the fit.

Despite these drawbacks, Eq. (8) is one of the few feasible approaches for describing many kinds of surfaces for systems with more than three atoms. This is especially true for surfaces for which DIM is not feasible or not accurate (a common situation) and for surfaces having multiple reaction paths (for which the methods to be described in the next section have serious difficulty). As a result, most of the >3-atom surfaces are based in some sense on Eq. (8), and we shall given some examples of this in Sec. IV.

D. Global surfaces based on reaction paths

Since *ab initio* methods can efficiently determine energy gradients and second derivatives, they are increasingly being used to determine the properties of *reaction paths.* Such paths are usually defined in terms of steepest-descents paths starting from saddle points, but here the precise definition will be left open. For a system with many degrees of freedom, often the only computationally feasible way to sample configuration space in *ab initio* calculations is to determine the potential along reaction paths, and since these paths usually play an important role in dynamics, it is necessary to consider the possibility of developing global surfaces from reaction-path information.

Actually, in some contexts the idea of defining surfaces in terms of reaction-path information has been successfully used for a long time. The best example is H atom addition reactions such as $H+C_2H_4$ (Hase *et al.*, 1978), where the reaction-path coordinate can simply be taken to be the C—H stretch. Hase and co-workers have developed a very general program known as MERCURY (Hase, 1980; Hase and Duchovic, 1985), which enables the representation of surfaces of this type (and also the study of trajectories on these surfaces). In this program, the molecular geometry and internal force field of the full molecule is allowed to vary parametrically with distance along the reaction path. Typically one uses hyperbolic tangent-switching functions to interpolate between values of internuclear distances, angles, force constants, etc., for the full molecule and for the dissociated fragments. Information needed to determine the parametric dependence is often available from *ab initio* calculations or may be derived from experiment. A recent example of a surface based on this approach is that for $H+CH_3$ (Duchovic *et al.*, 1984).

Unfortunately many reactive systems have more than one important reaction path, and many reaction paths involve the simultaneously breaking and forming of two or more bonds rather than just one bond, and in these cases the method described above for developing a global surface needs to be generalized. One obvious generalization, for systems with a single reaction path in which there is simultaneous breaking and forming of two or more bonds, is to define the reaction path so that it involves collective motion of two or more bond distances or other variables. (A steepest-descents path will do this.) It is then logical to represent the surface near this path using potential parameters (bond distances and force constants) that depend parametrically on this path, just as was done for the addition reactions. The well-known natural collision coordinate and reaction-path Hamiltonian approaches (Marcus, 1966; Miller *et al.*, 1980) provide general methods for doing this for steepest-descents paths. Unfortunately such approaches usually break down away from the path, since local orthogonal coordinate systems based on paths with curvature (i.e., paths involving collective motion of several coordinates) are almost always multiply valued somewhere, and in such regions the potential surface is not uniquely defined. It is possible to use very specialized coordinate systems that are both locally perpendicular to the path and globally orthogonal (Witriol *et al.*, 1977; Agmon and Levine, 1979), but such coordinates are functionally complicated and have not been developed for surfaces depending on three or more independent variables. A better procedure is to use global orthogonal coordinates that are not locally perpendicular to the path. A general formalism for developing

surfaces based on this idea has recently been presented (Jasien and Shepard, 1988), but no real surfaces have yet been developed using this formalism.

One simple example of a reaction-path-based surface that was developed using globally orthogonal coordinates not locally perpendicular to the path is the bond energy-bond order surface of Schatz *et al.* (1981) for $O(^3P)+H_2$. This surface used the configuration-space decomposition and coordinate systems of Fig. 1. In regions I and II the internuclear distances were used as coordinates, while in region-III polar coordinates were used. The region III path location and energy were determined from the bond-energy–bond-order (empirical) formulas (Johnston and Parr, 1963; Johnston, 1966). Force constants for *AB* and *BC* stretch motions at the path were then determined from Badger's (empirical) rule, and in region III these force constants were combined to define a radial force constant (in the l direction in Fig. 1), which it should be noted does not usually correspond to motions perpendicular to the reaction path. This force constant was then combined with the energy and geometry along the path and the energy and geometry at the swing point (see Fig. 1) to define a rotated Morse oscillator expression for the collinear potential surface. This surface was generalized to three dimensions by adding repulsive two-body potentials between the "end" atoms (i.e., the atoms that are farthest apart). This end-atom term arises naturally from the bond-energy–bond-order approach, but one could instead have used bending information defined along the reaction path to develop a three-dimensional surface, perhaps following the procedure of Joseph *et al.* (1988) to switch between surfaces in different arrangement channels.

III. CASE STUDIES OF SELECTED TRIATOMIC SURFACES

A. $O+H_2$

$O(^3P)+H_2$ is one of the most thoroughly studied atom-diatom reactions (for reviews, see Schatz, 1981, 1988b; Truhlar *et al.*, 1987). A large number of potential surfaces have been developed for it and Table I summarizes the most important of these. Included in this table are (1) commonly used acronyms by which we label the surfaces, (2) year the surface was published, (3) type of surface [LEPS, DIM, MBE (many-body expansion), RP (reaction-path-based surface), RMS], and (4) properties of the saddle point, including barrier height ($V^\ddagger$), OH and HH bond distances ($r^\ddagger_{OH}, r^\ddagger_{HH}$), and saddle-point symmetric stretch, bend, and asymmetric stretch frequencies ($\nu^\ddagger_s$, $\nu^\ddagger_b$, $\nu^\ddagger_a$). Note that all of the methods discussed in Sec. II have been used in developing surfaces. In addition, $O+H_2$ is one of the few reactions for which the reaction dynamics has been studied and compared on many of the surfaces, so it is appropriate to discuss it in detail. Before doing this we should point out that there are actually two reactive potential surfaces that correlate between $O(^3P)+H_2$ and $OH(^2\Pi)+H$, one of $^3A'$ symmetry and one of $^3A''$ symmetry. These two surfaces are degenerate for collinear geometry (the minimum-energy reaction path), and prior to 1981 only a single surface was commonly used to represent the two surfaces. Since 1981, the $^3A'$ and $^3A''$ surfaces have been separately determined. They differ by their saddle-point bend frequencies, which explains the double entries in Table I.

TABLE I. Properties of $O(^3P)+H_2$ surfaces.

Acronym	Year	Type of surface	$V^\ddagger$	$r^\ddagger_{OH}$	$r^\ddagger_{HH}$	$\nu^\ddagger_s$	$\nu^\ddagger_b$	$\nu^\ddagger_a$
LEPS-WDH[a]	1967	LEPS	0.510[i]	2.107[j]	1.798[j]	1538[k]	725[k]	1899i[k]
DIM[b]	1976	DIM	0.579	2.008	2.071	1736	417	1795i
LEPS-JW[c]	1977	LEPS	0.542	2.113	1.801	1533	725	1963i
SL[d]	1979	MBE	0.600	2.264	1.786	1535	698	1801i
BEBO[e]	1981	RP	0.500	2.111	1.815	1599	699	1622i
MOD-POLCI[f]	1981	RMS	0.546	2.293	1.739	1627	514[l] 1052	1800i
M2[g]	1986	RMS	0.546	2.293	1.739	1622	514[l] 836	1800i
J3[h]	1988	RMS	0.565	2.30	1.73	1631	512[l] 835	1847i

[a]Westenberg and deHaas (1967).
[b]Whitlock *et al.* (1976).
[c]Johnson and Winter (1977); Schatz (1985).
[d]Schinke and Lester (1979).
[e]Schatz *et al.* (1981).
[f]Schatz *et al.* (1981); Lee *et al.* (1982).
[g]Truhlar *et al.* (1984); Garrett and Truhlar (1986).
[h]Joseph *et al.* (1988).
[i]In eV.
[j]In a_0.
[k]In cm^{-1}.
[l]Top entry is for $^3A''$ surface, bottom for $^3A'$ surface.

As Table I shows, the first surfaces developed for $O+H_2$ were semiempirical: first a LEPS surface by Westenberg and de Haas (1967), then a DIM surface by Whitlock *et al.* (1976), and then a reparametrized LEPS by Johnson and Winter (1977; later revised by Schatz, 1985). The LEPS surfaces were derived by adjusting the Sato parameters to give transition-state theory or trajectory-rate coefficients that agreed with experiment. The DIM surface, on the other hand, is the direct result of a DIM calculation and was not fit in any sense to $O+H_2$ experiments. Figure 2 presents a contour plot of the LEPS-JW surface for collinear OHH geometries. A key feature of this surface is that the barrier is located rather centrally, with $r^{\ddagger}_{OH}/r^{e}_{OH}=1.15$ and $r^{\ddagger}_{HH}/r^{e}_{HH}=1.28$. From Table I we note that the DIM surface has a saddle point that, although similar in height, is different in location, being in the product region with $r^{\ddagger}_{OH}/r^{e}_{OH}=1.10$ and $r^{\ddagger}_{HH}/r^{e}_{HH}=1.48$. At the time these surfaces were first developed, it was unclear which of the two was more accurate, since both gave similar estimates of thermal rate coefficients (Schatz *et al.*, 1981). The subsequently developed bond-energy–bond-order surface (Schatz *et al.*, 1981) that was described in Sec. II.D gave a barrier close to the LEPS-JW one, but several surfaces derived from *ab initio* calculations have now shown that the correct barrier is even more reagentlike than LEPS-JW (though still centrally located).

Schinke and Lester (1979) were the first to develop a global $O+H_2$ surface based on a many-body expansion least-squares fit to the *ab initio* calculations of Howard *et al.* (1979). This surface had $r^{\ddagger}_{OH}/r^{e}_{OH}=1.24$ and $r^{\ddagger}_{HH}/r^{e}_{HH}=1.27$. A subsequent RMS surface developed by Schatz *et al.* (1981) and Lee *et al.* (1982) based on fits to slightly more accurate *ab initio* calculations has an even more reagentlike barrier. This surface (labeled MOD-POLCI) is plotted in Fig. 3.

A number of dynamics studies (Garrett, Truhlar, Bowman *et al.*, 1986; Bowman and Wagner, 1987, and references therein) have now shown that the productlike saddle point on DIM is incompatible with measured rates for the $O+H_2(v=1)$ reaction. The distinction between LEPS-JW and *ab initio* surfaces such as RMS is more subtle, but a combination of thermal rates, isotope effects, and vibrationally excited rates has been used to show that the *ab initio* surfaces are in better agreement with experiment (Wagner and Bowman, 1987).

Very recently, the accuracy of the *ab initio* calculations has been improved (Walch, 1987), and new isotope effects such as the (O+HD)/(O+DH) branching ratio have been measured (Robie *et al.*, 1987). In addition, rate coefficients have been measured over a wider range of temperatures than in the past (Presser and Gordon, 1985; Michael, 1988; Zhu *et al.*, 1988), so further refinements to the *ab initio* surfaces have become possible. The surfaces labeled M2 and J3 in Table I have resulted from this work (J3 being the latest). In these surfaces, the barrier height has been revised slightly, some of the spline terms have been modified relative to MOD-POLCI, and new algorithms for describing the bending dependence of the potential have been introduced (Truhlar *et al.*, 1984; Garrett and Truhlar, 1986; Joseph *et al.*, 1988). Based on variational transition-state theory [which should be accurate (Garrett, Truhlar, and Schatz, 1986; Haug *et al.*, 1987)], the new J3 surface describes all thermal rate information to within experimental uncertainty (Joseph *et al.*, 1988). Unfortunately J3 is not apparently a fully global surface (see Sec. II.A), so the ultimate $O+H_2$ surface remains to be developed.

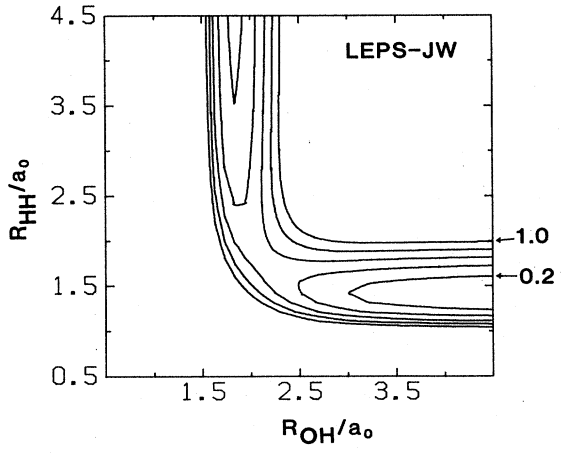

FIG. 2. Contour plot of LEPS-JW $O+H_2$ surface for linear O—H—H geometry as a function of the O—H and H—H distances (in a_0 units). Contours are in 0.2-eV intervals, starting at 0.2 eV, with zero taken to be separated $O+H_2$ with H_2 at equilibrium.

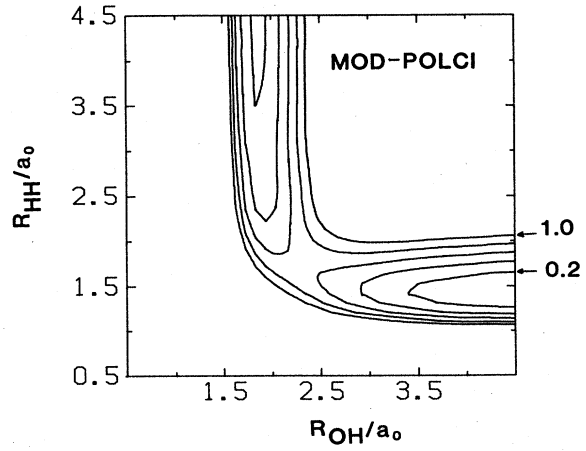

FIG. 3. Contour plot of MOD-POLCI surface for $O+H_2$ using same parameters as in Fig. 2.

TABLE II. Properties of Cl+HCl surfaces.

Acronym	Year	Type of surface	$V^{\ddagger}$	$\theta^{\ddagger}$	$r^{\ddagger}_{HCl}$	$\nu^{\ddagger}_s$	$\nu^{\ddagger}_b$	$\nu^{\ddagger}_a$
BCMR[a]	1983	LEPS	0.37[f]	180°	2.772[g]	344[h]	508[h]	1398i[h]
s-POLCI[b]	1983	RMS/QQ	0.33	161.4°	2.784	326	1619	1606i
DIM-3C[c]	1986	DIM	0.36	180°	2.86	360	256	1562i
PK2[d]	1987	LEPS	0.37	180°	2.793	343	612	1436i
PK3[d]	1987	LEPS	0.37	180°	2.811	345	691	1467i
sf-POLCI[e]	1988	RMS/QQ/LEPS	0.33	161.4°	2.784	326	1617	1606i

[a]Bondi *et al.* (1983).
[b]Garrett *et al.* (1983).
[c]Last and Baer (1986).
[d]Persky and Kornweitz (1987).
[e]Schatz *et al.* (1988).
[f]In eV.
[g]In a_0.
[h]In cm^{-1}.

B. Cl+HCl

$Cl(^2P)+HCl$ is an important prototype for reactions that involve the transfer of a light atom between two heavy atoms. In contrast to the case of $O+H_2$, there are few experimental data available (thermal rate coefficients at a few temperatures have been measured, as reviewed by Garrett *et al.*, 1983), so the several surfaces that have been developed have not been subjected to as much refinement as those for $O+H_2$. On the other hand, several high-quality theoretical dynamics studies have been carried out on several of the surfaces, and the dependence of dynamical results on certain features of the surfaces is known to be especially strong.

Table II summarizes the properties of several of the surfaces that have been developed for Cl+HCl. LEPS-type surfaces were in use prior to 1983 (Smith and Wood, 1973; Thommarson and Berend, 1973; Smith, 1975; Wilkins, 1975; Thompson, 1982), but most of these surfaces were not specifically optimized for Cl+HCl. Instead they were derived for the well-studied $H+Cl_2 \rightarrow HCl+Cl$ rearrangement that occurs on the same surface. The BCMR surface (Bondi *et al.*, 1983) was, however, explicitly optimized to fit Cl+HCl rate data. Figure 4 plots this surface for its most favorable (linear) reaction path.

At roughly the same time as BCMR, an *ab initio* calculation was carried out on Cl+HCl, and the resulting energies were used as the basis for the s-POLCI surface (Garrett *et al.*, 1983), which is plotted in Fig. 5. In this surface, an RMS function is used to describe linear geometries, and a quadratic/quartic (QQ) expansion in the bend angle is used to describe nonlinear geometries within 90° of linear. This surface has a nonlinear reaction path ($\theta^{\ddagger}=161.4°$), but is otherwise similar to BCMR in all properties except the bending frequency $\nu^{\ddagger}_b$. However, even this difference is more apparent than real, as

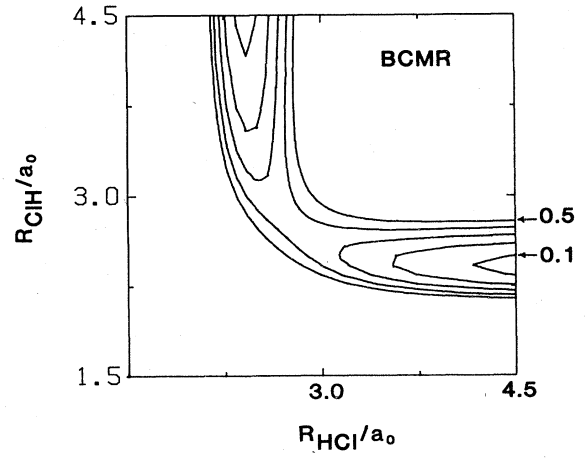

FIG. 4. Contour plot of BCMR Cl+HCl surface for linear Cl—H—Cl geometry as a function of the Cl—H and H—Cl distances (in a_0 units). Contours are in 0.1-eV intervals, starting at 0.1 eV, with zero taken to be separated Cl+HCl with HCl at equilibrium.

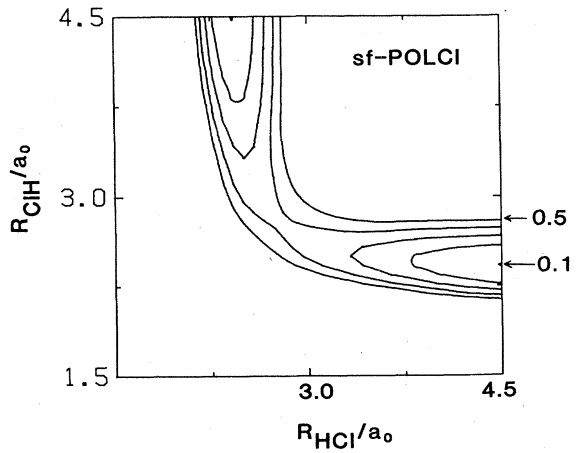

FIG. 5. Contour plot of s-POLCI (or equivalently sf-POLCI) Cl+HCl surface using same parameters as in Fig. 4.

the bend zero-point energies on the two surfaces are very close (Schatz *et al.*, 1988). Recently the *s*-POLCI surface has been generalized into a global surface (denoted *sf*-POLCI, Schatz *et al.*, 1988) by combining the *s*-POLCI for bend angles within 30° of collinear with a LEPS function which is similar to the BCMR surface. A dynamics study on this global surface (Schatz *et al.*, 1988) leads to cross sections and rate coefficients similar to those for the BCMR surface, indicating that the bent-geometry saddle point on *sf*-POLCI does not alter the reaction dynamics significantly compared to the linear-saddle-point BCMR.

The DIM-3*C* method has also been used to generate a potential surface for Cl+HCl (Last and Baer, 1986). As with the BCMR surface, this surface has a linear saddle point, but the saddle-point bend frequency on this surface is much lower than on BCMR. The dynamical consequences of this difference have not been carefully studied, but trajectory and approximate quantum studies on DIM-3*C* suggest (Abu Salbi *et al.*, 1984; Pollak *et al.*, 1985; Last and Baer, 1987) that the differential cross section in the backward direction oscillates as a function of energy, while trajectory and approximate and exact quantum results on BCMR (Amaee *et al.*, 1987; Schatz, 1988a) indicate that such "oscillating reactivity" effects do not occur.

The sensitivity of the Cl+HCl reaction dynamics to saddle-point bending frequency has been studied in detail by Persky and Kornweitz (1987) using three surfaces, PK1, PK2, and PK3, the first of which is essentially the same as BCMR, while the other two are identical to BCMR only for collinear geometries and have higher bend frequencies, as indicated in Table II. The different bending-angle dependence of the BCMR and PK3 surfaces is illustrated in Figs. 6 and 7, where we plot potential-energy contours for a fixed H—Cl distance of $2.8a_0$ as a function of the Cl—HCl (Cl atom to HCl

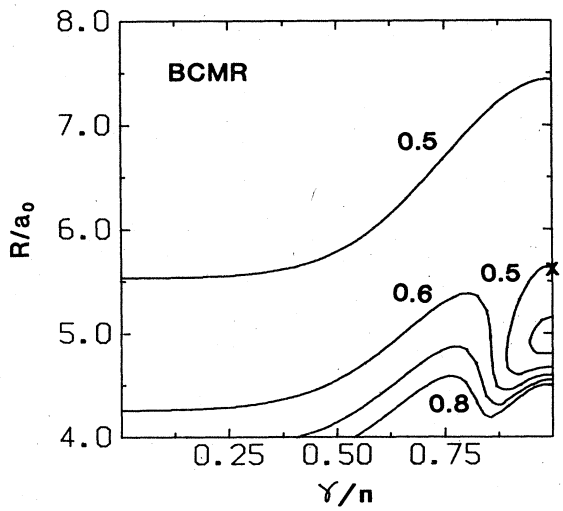

FIG. 6. Contour plot of BCMR Cl+HCl surface as a function of the Cl+HCl center-of-mass distance R and HCl rotational angle γ (defined such that $\gamma=\pi$ corresponds to linear ClHCl), taking the HCl distance to be $2.8a_0$. Contour energies are the same as in Fig. 4. The saddle point is located by a cross.

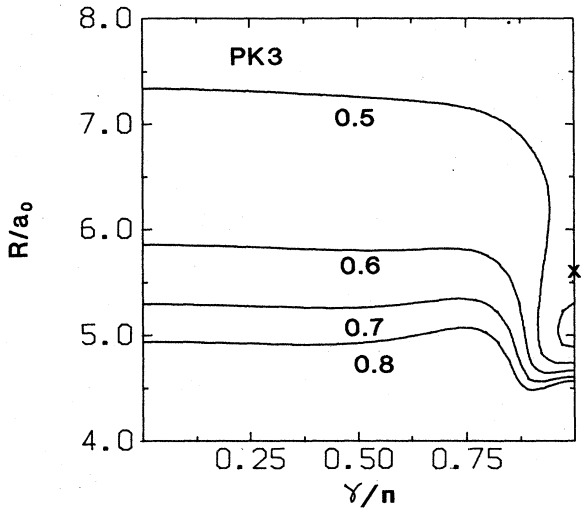

FIG. 7. Contour plot of PK3 Cl+HCl surface using same parameters as Fig. 6.

center of mass) distance R and the angle γ between the Cl—HCl and Cl—Cl vectors. $\gamma=\pi$ corresponds to the minimum-energy path for reaction, but note how the BCMR surface for each value of R is lower at $\gamma=0$ than at $\gamma=\pi$. There is a barrier between the $\gamma=0$ and $\gamma=\pi$ minima, but this is relatively small for R values down to the saddle point (the cross on Fig. 6). The PK3 surface, by contrast, is higher at small γ than at $\gamma=\pi$. The latter behavior forces the HCl to "lock" its orientation toward the incoming Cl prior to crossing the saddle point, while the former allows for free rotor motion (Amaee *et al.*, 1987; Loesch, 1987), and this leads to major differences in a number of dynamical features, including the energy dependence of the differential cross sections (Persky and Kornweitz, 1987) and rotational distributions (Schatz, 1987). Oscillating reactivity effects are seen on PK3 as a result of the "locked" orientation during reaction, since

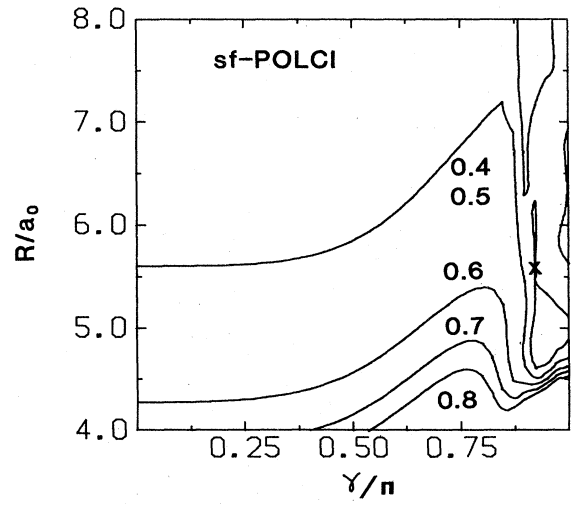

FIG. 8. Contour plot of *sf*-POLCI Cl+HCl surface using same parameters as Fig. 6.

the H atom can vibrate back and forth between the Cl's several times while the system is close to the saddle point. The BCMR surface, by contrast, shows no oscillations in differential cross section (Schatz *et al.*, 1987), since the H atom passes over the saddle point "sideways" (Amaee *et al.*, 1987). The *sf*-POLCI surface, which we plot in Fig. 8, is quite similar to BCMR, even though there is a shallow trough in the figure at $\gamma/\pi=0.9$, which corresponds to the nonlinear reaction path. It is unclear from this analysis why the DIM-3*C* surface, with its much lower bend frequency, should also show oscillating reactivity.

C. H+CO

H+CO→HCO is one of the simplest addition reactions, and it has been well studied from a number of different perspectives, as reviewed by Dunning *et al.* (1988). Small portions of the ground ($^2A'$) electronic surface have been characterized in a number of studies (as reviewed by Dunning, 1980), but only four attempts at developing a global surface have been made. Three of these surfaces (Carter *et al.*, 1979; Geiger and Schatz, 1984; Murrell and Rodriguez, 1986) are based on the MBE approach, and since they represent successive refinements within a given framework based on new *ab initio* data, only the latest one will be described. The fourth surface (Bowman *et al.*, 1985) was mentioned in Sec. II.A (where it was denoted BBH), and is based on a three-dimensional spline fit that is global except for the absence of O+CH and C+OH arrangement channels. It is significant to note that the latest MBE surface (which we label MR) was developed by fitting to several properties of the BBH surface. As a result, a comparison of these surfaces as well as of the dynamics on these surfaces will provide a sensitive test of the MBE fitting strategy.

Table III summarizes the properties of the minima and saddle points on the BBH and MR HCO potential surfaces. The presence of two minima (HCO, COH) and three saddle points (H · · · CO, CO · · · H, isomerization) makes the development of a global surface quite difficult and is one reason why the global-spline approach used by BBH is useful in this case. The table indicates, however, that the MR surface fits many of the BBH properties quite well. The MR fit to BBH was specifically designed to reproduce the geometry, energy, and force constants of the HCO minimum, the geometry and energy of the three saddle points, and the geometry, energy, and one force constant of the COH minima. All the specifically fit properties are accurately described by MR and, in ad-

TABLE III. Comparison of HCO minima and saddle points.[a]

Species	Parameters	BBH[b]	MR[c]
HCO minimum	V (relative to H+CO)	−0.841	−0.809
	R_{CH}	2.124	2.183
	R_{CO}	2.259	2.224
	HCO angle	124.2	123
	Harmonic frequencies	2749, 1908, 1157	2485, 1865, 1082
HCO saddle point	V	0.069	0.069
	R_{CH}	3.493	3.825
	R_{CO}	2.180	2.173
	HCO angle	117.2	124
	Harmonic frequencies	2121, 399, 598*i*	1945, 405, 611*i*
COH minimum	V	0.841	1.041
	R_{OH}	1.852	1.848
	R_{CO}	2.455	2.434
	COH angle	111.7	114
	Harmonic frequencies	3628, 1387, 1185	3162, 1456, 1046
COH saddle point	V	1.457	1.503
	R_{OH}	2.314	2.487
	R_{CO}	2.262	2.353
	COH angle	119.2	141
	Harmonic frequencies	2103, 980, 3130*i*	1117, 960, 1284*i*
Isomerization saddle point	V	2.107	2.301
	R_{CH}	2.493	2.512
	R_{CO}	2.453	2.438
	R_{OH}	2.165	2.154
	Harmonic frequencies	2519, 1464, 2305*i*	2956, 228, 1645*i*

[a]All distances are in Bohr, angles in degrees, frequencies in cm^{-1}, energies in eV.
[b]Bowman *et al.* (1985).
[c]Murrell and Rodriguez (1986); Chawla *et al.* (1988).

dition, many of the HCO and COH saddle-point frequencies match BBH quite closely, even though they were not specifically optimized. The most important differences arise in the COH and isomerization saddle points. For COH, the C—O stretch frequency is much too low on MR, as is the O—H stretch imaginary frequency. In addition, on MR the CO internuclear distance ($2.353a_0$) at the COH saddle point is closer to the COH minimum value ($2.434a_0$) than to isolated CO ($2.132a_0$), while on BBH, the CO distance at the COH saddle point ($2.26a_0$) is closer to isolated CO ($2.173a_0$) than to the COH minimum value ($2.455a_0$). At the isomerization saddle point, the CO stretch frequency is much lower on MR than on BBH (228 cm^{-1} versus 1464 cm^{-1}).

Figures 9 and 10 present contours of the BBH and MR surfaces for fixed CO distances taken to be the isolated CO equilibrium distances in each case. These figures show that the two surfaces have the same global shape and stationary points. The most noticeable quantitative difference arises in how quickly the potential falls off for geometries perpendicular to the C—O axis.

The most extensive comparisons between *dynamics* on the BBH and MR potentials have been in studies of collisional excitation of CO by translationally hot H atoms (1–4 eV collision energy). The earliest experimental studies of this were restricted to examining vibrational excitation (Wight and Leone, 1983a, 1983b): Trajectory studies on both BBH (Geiger *et al.*, 1985) and MR (Murrell and Rodriguez, 1986) surfaces were able to reproduce the measured vibrational distributions quite accurately. Recently, Chawla *et al.* (1988) have extended these measurements to include rotational distributions for both elastic and vibrationally inelastic scattering, and

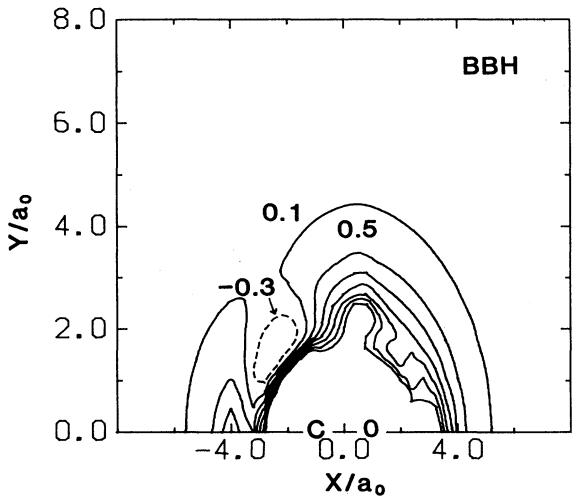

FIG. 9. Contour plot of BBH H+CO surface as a function of the x and y coordinates of the H atom, relative to the CO center of mass. The CO is fixed on the x axis (O atom to the right), with the C—O distance taken to be the isolated CO equilibrium value. Contours are in 0.4-eV intervals, with the lowest at −0.3 eV relative to isolated H+CO.

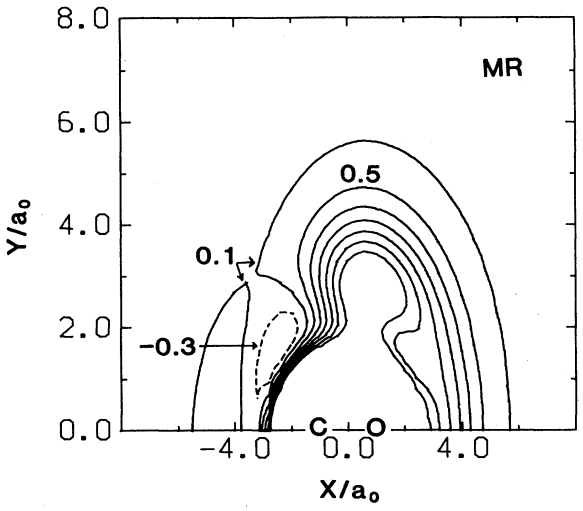

FIG. 10. Contour plot of MR H+CO surface using the same parameters as in Fig. 9.

they find that only BBH predicts results that match their measurements. MR was found to give too large a vibrationally inelastic ($v=1$) cross section for low rotational quantum states ($j<15$) as a result of a subtle difference between BBH and MR that is not apparent from Figs. 9 and 10. This difference is found in examining the derivatives of the two surfaces with respect to the CO stretch coordinate, which we plot in Figs. 11 (BBH) and 12 (MR). This derivative is the key source of coupling responsible for vibrational excitation, and we see from the figure that the derivative is larger at longer range near the COH saddle point on MR than on BBH. This is also apparent from the location of the COH saddle point in

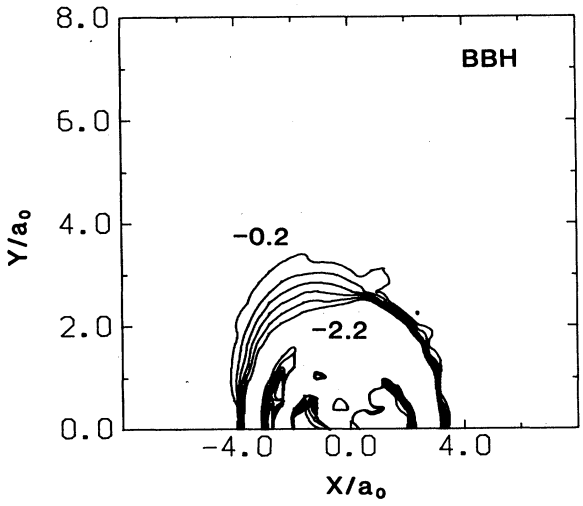

FIG. 11. Contour plot of derivative of BBH H+CO surface with respect to C—O distance. Contours are in intervals of 0.4 eV/a_0, from -2.2 eV/a_0 to -0.2 eV/a_0.

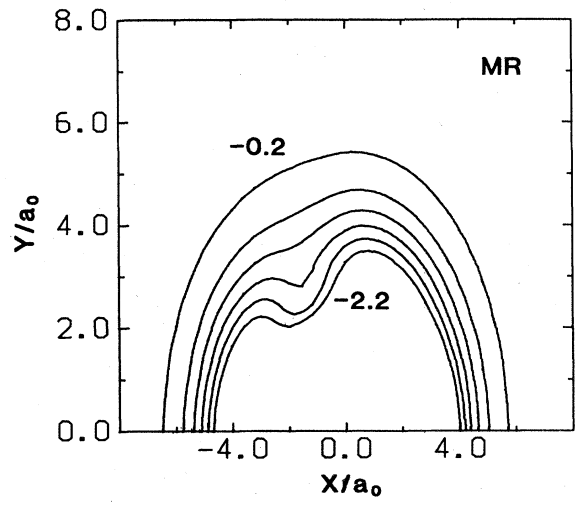

FIG. 12. Contour plot of derivative of MR surface as in Fig. 11.

Table III, which, as noted earlier, occurs for longer CO distances on MR than on BBH. An analysis of the trajectories shows that this difference between the derivatives is responsible for the excessively large vibrational excitation cross section (factor of 2.5).

This unfortunate result for the MR surface graphically illustrates how sensitive vibration/rotation energy transfer results are to features of potential surfaces. It also shows how difficult it can be to determine global potential surfaces of acceptable accuracy (even for a relatively "simple" surface) by fitting locally defined surface features.

D. H_2O [$O(^1D)+H_2 \rightarrow OH(^2\Pi)+H$]

H_2O is, of course, one of the most important and most often used potential surfaces. A complete review of all of the H_2O ($^1A'$) surfaces that have been developed is beyond the scope of this paper, but if we restrict our consideration to global surfaces that dissociate correctly and that therefore describe the reaction $O(^1D)+H_2 \rightarrow OH(^2\Pi)+H$, then the number of such surfaces that have been developed is surprisingly small. Table IV summarizes those developed since 1976, including values of the energies associated with the H_2O equilibrium, separated $O(^1D)+H_2$, and separated $OH(^2\Pi)+H$. Before discussing these surfaces we should note that although the $H_2O(^1A')$ surface is well below $H_2O(^3A'$ and $^3A'')$ (i.e., the $O+H_2$ surfaces of Sec. III.D) near equilibrium, it is well above them for separated $O(^1D)+H_2$ geometries and is degenerate with them for separated $OH(^2\Pi)+H$ (see Durand and Chapuisat, 1985). The crossing of the singlet and triplet surfaces in the $O+H_2$ arrangement channel has been examined in detail (Whitlock *et al.*, 1976), and there is no evidence that this crossing plays a role in either the singlet or triplet surface dynamics. As a result we shall ignore the triplet surfaces in our discussions.

The surfaces in Table IV can be divided into three groups: (a) MBE-type surfaces, which are based on fits to polynomial force fields for H_2O and to experimentally derived diatomic potentials for the asymptotes, (b) MBE surfaces, which are based on least-squares fits to global *ab initio* calculations, and (c) DIM surfaces. The SM, RS, and MC surfaces (see acronyms in Table IV) belong to type (a), SL1, SL3, MCMG, and MSL1 to type (b), and WMF and KNS (which actually denote three very similar surfaces that will not be distinguished here) to type (c).

The SM surface was the first MBE surface for H_2O, and it was based on fits to an empirically derived H_2O quartic force field (Hoy *et al.*, 1972). The RS surface represented a reparametrization of SM based on an *ab initio* quartic force field (Bartlett *et al.*, 1979). Both SM and RS have a cusp at an H—H distance of $3.157a_0$ due to a switch between surfaces (both of $^1A'$ symmetry)

TABLE IV. Global $H_2O(^1A')$ surfaces.

Acronym	Year	Type of surface	V_{H_2O}	V_{O+H_2}	V_{OH+H}
SM[a]	1976	MBE	−10.07[i]	−2.78[i]	−4.63[i]
SL1[b]	1980	MBE	−8.95	−1.87	−4.04
SL3[b]	1980	MBE	−8.93	−1.87	−4.04
RS[c]	1981	MBE	−10.07	−2.78	−4.63
MCMG[e]	1981	DMBE	−10.33	−2.78	−4.63
WMF[e]	1982	DIM	−9.16	−2.78	−4.58
MC[f]	1984	MBE	−10.07	−2.78	−4.63
MSL1[g]	1984	MBE	−8.95	−2.25	−4.03
KNS[h]	1988	DIM	−10.07	−2.78	−4.62

[a]Sorbie and Murrell (1976).
[b]Schinke and Lester (1980).
[c]Redmon and Schatz (1981).
[d]Murrell *et al.* (1981).
[e]Whitlock *et al.* (1982).
[f]Murrell and Carter (1984).
[g]Schinke (1984).
[h]Kuntz *et al.* (1988).
[i]In eV.
[j]Result is for the model 1 surface of Kuntz *et al.* (1988).

correlating to $O(^1D)+H_2(^1\Sigma_g^+)$ (appropriate for shorter H—H distances) and to $O(^3P)+H_2(^3\Sigma_u^+)$ (appropriate for larger distances). This cusp is rigorously present for infinite O—H_2 separation, but should be smoothed out for finite separation. Neither the SM nor the RS surface is completely smooth or continuous, however, and this makes it difficult to use these surfaces in trajectory calculations. To remedy this problem, Murrell *et al.*, (1981) introduced the idea of a double many-body expansion (DMBE) to represent the H_2O surface in which both the ground and excited singlet surfaces correlating to $O(^1D)+H_2(^1\Sigma_g^+)$ and to $O(^3P)+H_2(^3\Sigma_u^+)$ are fit simultaneously as a 2×2 determinant. The diagonal terms are represented using Eq. (8), and a similar off-diagonal term is introduced to describe the coupling between these two surfaces that leads to smoothing out of the cusp at finite O—H_2 separation. The resulting MCMG surface was fit to global *ab initio* calculations, and a subsequent trajectory study of the $O(^1D)+H_2$ reaction dynamics (Dunne and Murrell, 1983) produced accurate results for a number of properties. Since most interest in the H_2O surface is associated with energies that do not access the cusp region, Murrell and Carter (1984) developed a simpler alternative to MCMG that involves a single MBE [i.e., Eq. (8)] with the cusp smoothed out for all O—H_2 separations. Figure 13 shows a contour plot of the MC surface as a function of oxygen atom location for H_2 at its equilibrium geometry. This plot shows that the MC surface is downhill for all approaches of O to H_2, with the most favorable approach geometry being collinear. We shall compare this surface with other H_2O surfaces below.

SL1, SL3, and MSL1 surfaces are three of several surfaces that were developed by Schinke and Lester (1980) based on fits to the accurate global *ab initio* calculations of Howard *et al.* (1979). These fits used the MBE functional form in Eq. (10) (with a few adjustments), but the reference coordinates r_i' were chosen inside the equilibrium position and the multinomial coefficients were determined by least-squares fits that were designed to be globally rather than locally accurate. The SL1 and SL3 surfaces are, in fact, somewhat different fits to the same *ab initio* points that are of roughly comparable quality. They differ at large O—H_2 separation, where SL1 has a 0.05-eV barrier to addition for collinear geometry, while SL3 has no barrier. Figure 14 shows contour plots of the SL3 surface, using the same coordinates as in Fig. 13. The MC and SL3 surfaces are clearly very different, with SL3 having a most favored perpendicular geometry reaction path and much larger energy release for H_2 at its equilibrium geometry.

Table IV shows that the SL1, SL3 surfaces also differ from the empirically derived surfaces such as CM in the dissociation energies of H_2O, OH, and H_2. The difference is due to inaccuracies in the *ab initio* calculations; a further defect of SL1 and SL3 is that the H_2O, OH, and H_2 force fields are not very well described. These errors in dissociation energies and force fields lead to a number of problems, one of which is an incorrect partitioning of energy to the products of the $O(^1D)+H_2\rightarrow OH+H$ reaction (Schinke and Lester, 1980). To partially correct this error, Schinke (1984) added a correction term to SL1, leading to the modified SL1 (MSL1) surface, which has the correct exoergicity for the $O(^1D)+H_2\rightarrow OH+H$ reaction, but the other errors in SL1 were not corrected.

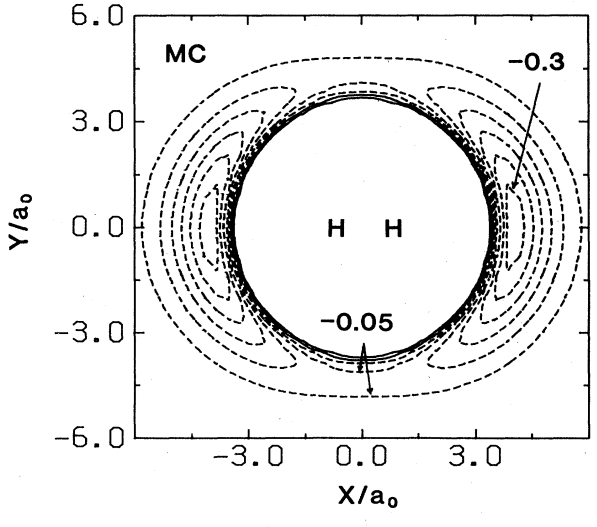

FIG. 13. Contour plot of MC H_2O surface as a function of the x and y coordinates of O relative to H—H center of mass, with H—H taken to be at equilibrium and on the x axis. Contours are in intervals of 0.05 eV, starting at −0.4 eV.

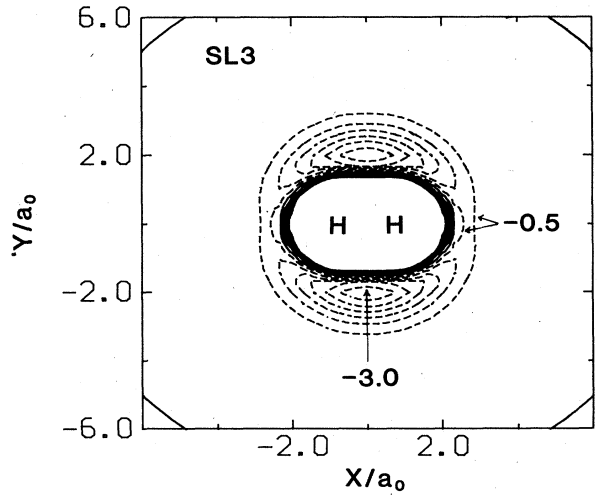

FIG. 14. Contour plot of SL3 H_2O surface using same parameters as in Fig. 13 except that contours start at −3.0 eV and are in 0.5-eV intervals.

Despite the many inaccuracies associated with SL1, SL3, and MSL1, recent highly accurate *ab initio* calculations (Bauschlicher and Taylor, 1986; Walch and Harding, 1988) have confirmed the qualitative accuracy of these surfaces. In particular, the *ab initio* study by Walch and Harding of the region of the surface pictured in Figs. 13 and 14 has shown that the most favored reaction path is perpendicular, as in Fig. 14. In addition, the linear O—H_2 approach has a very small barrier (<0.01 eV), which would probably vanish for a still larger calculation. In this respect, the correct surface is probably closer to SL3 (which has no collinear barrier) than to the other existing surfaces. Dynamics studies of $O(^1D)+H_2$ on MSL1 have successfully explained a number of measurements, with the only major unexplained piece of data being the OD/OH isotope ratio in O+HD (Fitzcharles and Schatz, 1986). Since SL3 is a slightly better surface than SL1, an important task for the future will be reparametrizing the SL3 surface so as to incorporate the recent *ab initio* calculations, a better H_2O force field, and correct OH and H_2 diatomic properties.

The DIM surfaces for H_2O have been developed by Whitlock *et al.* (1982) and by Kuntz *et al.* (1988). WMF was based on a five-state description of the electronic structure (meaning that a 5×5 determinant must be evaluated for each geometry). Although this surface describes OH and H_2 correctly, Table IV indicates that the H_2O dissociation energy is too small by about 1 eV. In addition, the H_2O force field is poorly described (Whitlock *et al.*, 1987), and studies of the $O(^1D)+H_2$ reaction dynamics have revealed some important inadequacies of WMF (Fitzcharles and Schatz, 1986). The KNS surface (a 9×9 determinant) represents an important improvement to the DIM description of H_2O that, while still far from perfect in the description of the H_2O force field, has the right energetics and is able to describe the $O(^1D)+H_2$ reaction dynamics correctly (Kuntz *et al.*, 1988). The OD/OH isotope ratio has not yet been considered on this surface.

One last surface that we would like to discuss for H_2O is one developed by Reimers and Watts (1984), the correct parameters for which are given by Barnett *et al.* (1988). This surface has been widely used for molecular dynamics studies of liquid water and as a building block for developing water cluster potential surfaces. However, it is not a proper global surface, even though it is expressed in terms of globally defined functions. The actual functional form is a sum of Morse functions:

$$V(R_1,R_2,\theta)=\sum_{i=1}^{3} D_i[1-\exp(-\alpha_i S_i)]^2 , \tag{11}$$

where R_1 and R_2 are the two OH distances and θ is the bend angle. D_i and α_i are parameters, and the coordinates S_i are given by

$$S_i=R_i\cos[(\theta-\theta_e)/2]-R_e \quad (i=1,2) , \tag{12a}$$

$$S_3=[(R_1+R_2)/R_e]\sin[(\theta-\theta_e)/2] , \tag{12b}$$

where θ_e and R_e are the equilibrium values of R_i ($i=1,2$) and θ, respectively.

The Morse parameters in this surface were determined by fitting measured vibrational energy levels of H_2O, D_2O, and HDO, and it does an excellent job in this respect. However, if Eq. (11) is evaluated in the limit that one of the R_i's is infinite, the resulting potential still depends on θ, even though it should not. This sort of defect is common in potentials that were specifically designed to describe a local region even though they are formally global.

IV. POTENTIAL-ENERGY SURFACES FOR $n>3$ POLYATOMIC MOLECULES: $H+CO_2$

There are very few global potential surfaces for molecules with more than three atoms that are realistic for all geometries. For most of the fitting methods in Sec. II, this problem arises from the fact that *ab initio* calculations cannot be performed for enough geometries to define the surfaces globally. For a few very special cases, such as the surface for $H_2^+ + H_2$, DIM theory is accurate and easy to apply, and thus global surfaces of acceptable accuracy are possible, but these cases are rare. Sometimes single reaction-path surfaces can be developed by applying the methods of Sec. II.D, but these surfaces are usually not global (though they may describe a subset of processes relevant to a given system accurately). Global spline approaches are obviously not feasible, so the most common approach to the surface fitting of polyatomics is the many-body expansion method of Eq. (8). It should be noted that this method can be implemented in a number of different ways other than by defining many-body potentials through Eq. (10). We include these other possibilities as still within the MBE framework.

Several $n>3$ polyatomic molecule potential surfaces have been developed in recent years based on the MBE approach (or combinations of MBE and RP). Among those not described in the Truhlar *et al.* review are $H+CO_2$ (Schatz *et al.*, 1987), $H+C_2H_2$ (White and Schatz, 1984), CH_3+H_2 (Steckler *et al.*, 1987; Joseph *et al.*, 1987), $F_2+C_2H_4$ (Raff, 1987), $SiH_2+SiH_2\rightarrow Si_2H_4$ (Agrawal *et al.*, 1988), and $CH_3CN\rightarrow CH_3NC$ (Sumpter and Thompson, 1987).

We shall now illustrate the practice and pitfalls of fitting surfaces using the MBE method by examining $H+CO_2$.

$H+CO_2$ and its reverse, OH+CO, are both important reactions in combustion (especially the reverse), and recently a number of measurements pertaining to state-to-state chemistry in these two reactions have been made, as summarized by Schatz *et al.* (1987). In addition, the structure and vibrational spectroscopy of the stable molecule HOCO, and the search for the still undetected molecule HCO_2, have been actively pursued (Jacox, 1987). The several minima and saddle points believed to be present on the HCO_2 potential surface are indicated in Fig. 15, along with estimates (Schatz *et al.*, 1987) of the

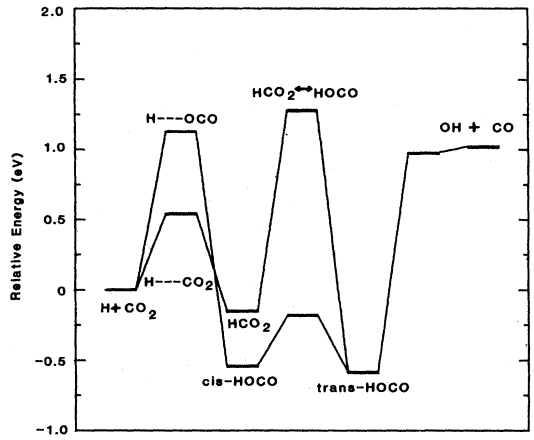

FIG. 15. Energies of minima and saddle points of $H+CO_2$ potential surface based on best estimates from Schatz *et al.* (1987).

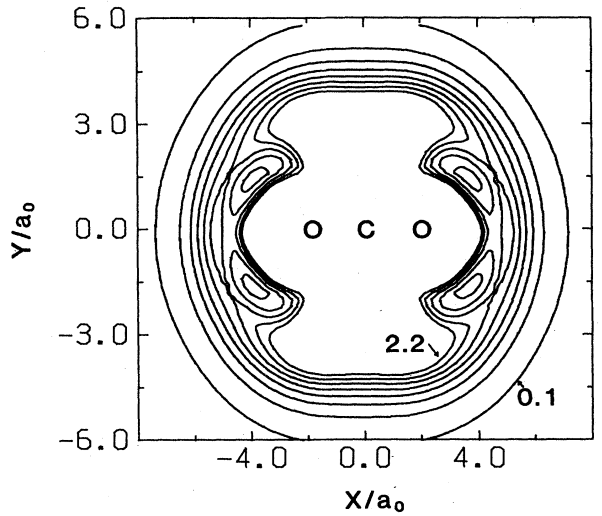

FIG. 16. Contour plot of two- and three-body part of SFH $H+CO_2$ potential surface as a function of x and y coordinates of H atom relative to CO_2 center of mass, with energy minimized with respect to CO_2 stretch and bend coordinates, subject to the constraint that the O—O bond be parallel to the x axis. Contours are in 0.3-eV intervals with lowest at -0.5 eV relative to separated $H+CO_2$ with CO_2 at equilibrium.

energy of each.

The global surface that has been developed for $H+CO_2$ was the work of Schatz, Fitzcharles, and Harding (SFH), and it involved a combination of fits to *ab initio* calculations and empirical adjustments within the MBE framework. A key factor underlying the feasibility of this surface is the existence of realistic potentials for the diatomic and triatomic fragments: OH, CH, HCO (Murrell and Rodriguez, 1986); CO, OO, CO_2 (Carter and Murrell, 1987); and HO_2 (Melius and Blint, 1979). This enables the surface to be written as

$$V=V^{(2)}_{CO}+V^{(2)}_{CO'}+V^{(2)}_{OH}+V^{(2)}_{O'H}+V^{(2)}_{OO'}+V^{(2)}_{CH}+V^{(3)}_{HCO}+V^{(3)}_{HCO'}+V^{(3)}_{HOO'}+V^{(3)}_{COO'}+V^{(4)} \quad (13)$$

with all the terms except $V^{(4)}$ known based on earlier work. If $V^{(4)}$ is simply neglected, then the surface plotted in Fig. 16 is obtained. In this plot, x and y are the H atom locations relative to the CO_2 center of mass, and for each x,y the energy has been minimized with respect to the CO_2 internal coordinates, with the constraint that the O—O′ axis be parallel to x. This surface shows a number of qualitatively correct features and a few incorrect ones. The HOCO minimum is present, but it is approximately 1.5 eV higher than it should be, and the CO_2 at this minimum is linear, so that the *cis* and *trans* isomers are not distinguished. The $H\cdots OCO$ addition saddle point is present, but the HCO_2 minimum and associated saddle points are completely missing.

It is useful to note that the surface plotted in Fig. 16 has two problems that are not apparent from this figure, which reveal how difficult it can be to define even the two- and three-body parts of $H+CO_2$ accurately. One is that $V^{(3)}_{HCO}$ and $V^{(3)}_{HCO'}$ are based on the MR surface for H+CO that was shown earlier (Sec. III.C) to have several incorrect features. The $H+CO_2$ surface of Schatz *et al.* (1987) was developed prior to the discovery of errors in the H+CO surface (see Chawla *et al.*, 1988), but even today there is no alternative, as the more accurate BBH surface for H+CO is not globally defined (does not describe C—O bond breakage). The second problem concerns the achievement of proper electronic symmetry for all geometries. The CO_2 potential surface from Carter and Murrell (1984) assumes that spin is conserved, so CO_2 dissociates to $CO(^1\Sigma)+O(^1D)$ (i.e., an excited oxygen atom). However, the ground state of HCO_2 dissociates to $CO(^1\Sigma)+O(^3P)+H(^2S)$ (i.e., a ground-state oxygen atom). As a result, direct use of the Carter and Murrell potential leads to dissociation to an excited state. To remedy this problem, SFH refit the CO_2 potential to a function that dissociates to $O(^3P)+CO(^1\Sigma)$. The function used is smooth, but in reality a cusp would be expected in view of the negligible coupling between the CO_2 singlet and triplet surfaces.

Now let us consider the fitting of the four-body term $V^{(4)}$. The approach of SFH was to use the 4-atom version of Eq. (10) to fit HCO_2 and HOCO minima that were determined from *ab initio* calculations. In these fits, Gaussian rather than hyperbolic tangent-switching functions were used, so that the minima could be added separately without interfering with each other. The $H\cdots OCO$, $H\cdots CO_2$, and isomerization saddle points of Fig. 15 were then added in by scaling the potential along reaction paths between each appropriate minimum or asymptote. With this procedure it was possible to adjust each saddle-point energy to desired values, but the geometry and vibrational frequencies were in some cases in error by substantial amounts compared to *ab initio* calculations. To adjust geometries, a mapping transformation was introduced which converts the coordinates into

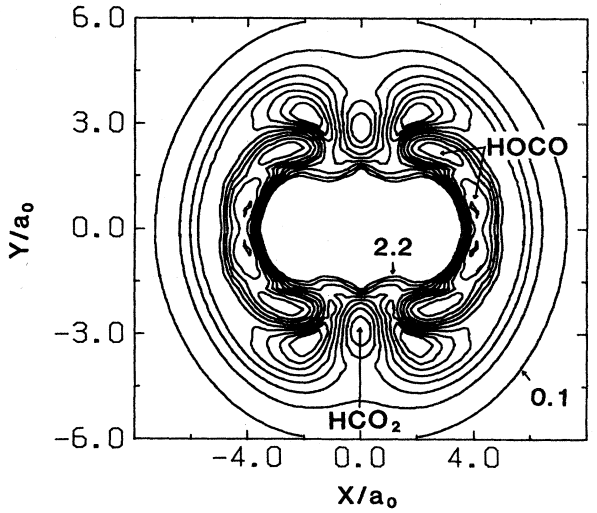

FIG. 17. Contour plot of complete SFH $H+CO_2$ potential surface using same parameters as in Fig. 16. Locations of the HOCO and HCO_2 minima are indicated, with the *cis* and *trans* isomers of HOCO appearing as two separate minima (*cis* is closer to the HCO_2 minimum).

new variables in desired regions in such a way as to move stationary points without changing surface topology. To adjust frequencies, additional localized functions were added which change selected force constants in desired regions without changing other properties.

The resulting global surface is plotted in Fig. 17 using the same coordinates as Fig. 16. Figure 17 shows a number of improvements over Fig. 16, including the correct appearance of all minima and saddle points, each having the energies indicated in Fig. 15. The geometries are mostly close to *ab initio* values, as are the frequencies of all minima. In addition, for saddle points, the sum of the frequencies, excluding the imaginary one, is close to the *ab initio* estimate. This constraint keeps the saddle-point harmonic zero-point energies close to their desired values.

The surface plotted in Fig. 17 has been tested by SFH in dynamical studies of $H+CO_2$ using classical trajectories. Both nonreactive collisional excitation and reaction to give $OH+CO$ have been considered, and the results have been mixed. Collisional excitation leads to cross sections from vibrational excitation that are too high, with too little rotational excitation. The reactive cross sections and product OH rotational distributions, by contrast, are in good agreement with experiment. It appears likely that the problems with collisional excitation are due to the problems with the HCO three-body surface discussed above, since similar studies of the $H+CO$ dynamics on this three-body surface led to excessively large vibrational excitation cross sections.

V. CONCLUSIONS

It is useful to summarize the status of each of the surfaces discussed in Secs. III and IV, as this illustrates both how well known these surfaces are and how difficult it is to determine accurate global potential surfaces. For $O(^3P)+H_2$, surfaces that describe all known features of the reaction dynamics exist, but the best of these surfaces ($J3$) is not really global in the sense of describing all three arrangement channels everywhere. Less is known experimentally about $Cl+HCl$, but several semiempirical and RMS surfaces have been developed that are consistent with the data. Theoretical dynamics studies indicate strong sensitivity of certain measurables to features of the potential surface, so the possibility of further improvement is good. For both $O(^3P)+H_2$ and $Cl+HCl$, high-quality *ab initio* surfaces are available only at a small number of geometries, so much is known of the surfaces only from interpolation using LEPS or other functions.

$H+CO$ is one of the few systems in which the surface is globally known based on three-dimensional spline fits to extensive *ab initio* calculations, but even this surface (BBH) is deficient in that it does not describe the dissociation of HCO to form $C+OH$ or $O+CH$. A simple MBE surface (MR), which was designed both to fit the BBH surface and to allow for dissociation to $C+OH$ and $O+CH$, turns out to have experimentally distinguishable errors in its C—O derivative for certain geometries. Thus it would be highly desirable to generate an improved global surface for $H+CO$.

Although a large number of H_2O potential surfaces have been developed, the "ultimate" surface is still missing. Existing MBE fits to global *ab initio* calculations appear to be qualitatively correct, but these surfaces need to be reparametrized to build in the correct H_2O force field and dissociated diatomic properties. Several MBE surfaces based on local fits to H_2O quartic force fields have been developed, but all of these have incorrect angular behavior at long range in the $O(^1D)+H_2$ region. The latest DIM surface (KNS) appears to be qualitatively correct everywhere, so it might be that with modest corrections a quantitatively accurate surface will be possible. This would be very helpful, since DIM has the advantage of automatically including surface crossing effects.

Finally $H+CO_2$ is an extremely difficult surface to represent, as a result of many minima and saddle points. A first attempt at developing a surface has been made, and this surface has many of the desired attributes. Unfortunately certain features are incorrect, so further revisions are needed. It is encouraging that the parts of the surface where four-body terms are important are all spatially localized. This allows relatively simple functions to be used in representing $V^{(4)}$, though no systematic procedure exists for selecting what these functions should be.

Perhaps the most important overall conclusion from this review of potential surface representations is that the technology for generating global potential surfaces is still in a relatively primitive state, which is often the limiting factor in developing theoretical interpretations of experiments. A number of approaches exist for generating potential surfaces, but those that have the most physical

content built in (i.e., the semiempirical methods) are rarely accurate enough to provide a useful starting point from which improved surfaces can be derived, while those that have the simplest mathematical structure [splines, many-body expansions based on Eq. (10)] can be inaccurate (even unphysical) unless a high density of global *ab initio* points is available for fitting. This problem could be circumvented if *ab initio* calculations were accurate and cheap enough to do at every geometry needed for dynamics studies, but this possibility seems unlikely for the foreseeable future using existing technology.

ACKNOWLEDGMENTS

This research was supported by NSF Grant No. CHE-8715581. I thank Jonathan Connor and Albert Wagner for several valuable discussions concerning this work.

REFERENCES

Abu Salbi, N., S-H. Kim, D. J. Kouri, and M. Baer, 1984, Chem. Phys. Lett. **112**, 502.
Agmon, N., and R. D. Levine, 1979, J. Chem. Phys. **71**, 3034.
Agrawal, P. M., D. L. Thompson, and L. M. Raff, 1988, J. Chem. Phys. **88**, 5948.
Amaee, B., J. N. L. Connor, J. C. Whitehead, W. Jakubetz, and G. C. Schatz, 1987, Faraday Discuss. Chem. Soc. **84**, 387.
Baer, M., and I. Last, 1981, in *Potential Energy Surfaces and Dynamics Calculations,* edited by D. G. Truhlar (Plenum, New York), p. 519.
Barnett, R. N., U. Landman, C. L. Cleveland, and J. Jortner, 1988, J. Chem. Phys. **88**, 4421.
Bartlett, R. J., I. Shavitt, and G. D. Purvis, 1979, J. Chem. Phys. **71**, 281.
Bauschlicher C. W., Jr., and P. R. Taylor, 1986, J. Chem. Phys. **85**, 2779.
Bender, C. F., B. J. Garrison, and H. F. Schaefer, 1975, J. Chem. Phys. **62**, 1188.
Bondi, D. K., J. N. L. Connor, J. Manz, and J. Romelt, 1983, Mol. Phys. **50**, 467.
Botschwina, P., and W. Meyer, 1977, Chem. Phys. **20**, 43.
Bowman, J. M., J. S. Bittman, and L. B. Harding, 1985, J. Chem. Phys. **83**, 660.
Bowman, J. M., and A. Kuppermann, 1975, Chem. Phys. Lett. **34**, 523.
Bowman, J. M., and A. F. Wagner, 1987, J. Chem. Phys. **86**, 1967.
Bowman, J. M., A. F. Wagner, S. P. Walch, and T. H. Dunning, Jr., 1984, J. Chem. Phys. **81**, 1739.
Brown, F. B., R. Steckler, D. W. Schwenke, D. G. Truhlar, and B. C. Garrett, 1985, J. Chem. Phys. **82**, 188.
Carter, S., I. M. Mills, and J. N. Murrell, 1979, J. Chem. Soc. Faraday Trans. 2 **1**, 148.
Carter, S., and J. N. Murrell, 1984, Croat. Chem. Acta **57**, 355.
Chapman, S., M. Dupuis, and S. Green, 1983, Chem. Phys. **78**, 93.
Chawla, G. K., G. C. McBane, P. L. Houston, and G. C. Schatz, 1988, J. Chem. Phys. **88**, 5481.
Connor, J. N. L., 1979, Comput. Phys. Commun. **17**, 117.
Daw, M. S., and M. I. Baskes, 1984, Phys. Rev. B **29**, 6443.
Duchovic, R. J., W. L. Hase, and H. B. Schlegel, 1984, J. Phys. Chem. **84**, 1339.
Dunne, L. J., and J. N. Murrell, 1983, Mol. Phys. **50**, 635.
Dunning, T. H., Jr., 1980, J. Chem. Phys. **73**, 2304.
Dunning, T. H., Jr., and L. B. Harding, 1985, in *Theory of Chemical Reaction Dynamics,* edited by M. Baer (CRC Press, Boca Raton, FL), Vol. 1, p. 1.
Dunning, T. H., Jr., L. B. Harding, A. F. Wagner, G. C. Schatz, and J. M. Bowman, 1988, Science **240**, 453.
Durand, G., and X. Chapuisat, 1985, Chem. Phys. **96**, 381.
Eaker, C. W., and C. A. Parr, 1976, J. Chem. Phys. **64**, 1322.
Ellison, F. O., 1963, J. Am. Chem. Soc. **85**, 3540.
Fitzcharles, M. S., and G. C. Schatz, 1986, J. Phys. Chem. **90**, 3634.
Garrett, B. C., and D. G. Truhlar, 1986, Int. J. Quantum Chem. **29**, 1463.
Garrett, B. C., D. G. Truhlar, J. M. Bowman, A. F. Wagner, D. Robie, S. Arepalli, N. Presser, and R. J. Gordon, 1986, J. Am. Chem. Soc. **108**, 3515.
Garrett, B. C., D. G. Truhlar, and G. C. Schatz, 1986, J. Am. Chem. Soc. **108**, 2876.
Garrett, B. C., D. G. Truhlar, A. F. Wagner, and T. H. Dunning, Jr., 1983, J. Chem. Phys. **78**, 4400.
Geiger, L. C., and G. C. Schatz, 1984, J. Phys. Chem. **88**, 214.
Geiger, L. C., G. C. Schatz, and L. B. Harding, 1985, Chem. Phys. Lett. **114**, 520.
Gittens, M. A., D. M. Hirst, and M. F. Guest, 1977, Faraday Discuss. Chem. Soc. **62**, 67.
Gray, S. K., and J. S. Wright, 1977, J. Chem. Phys. **66**, 2867.
Hase, W. L., 1980, Quantum Chem. Program Exchange **11**, 453.
Hase, W. L. and R. J. Duchovic, 1985, J. Chem. Phys. **83**, 3448.
Hase, W. L., G. Mrowka, R. J. Brudzynski, and C. S. Sloane, 1978, J. Chem. Phys. **69**, 3548.
Haug, K., D. W. Schwenke, D. G. Truhlar, Y. Zhang, J. Z. H. Zhang, and D. J. Kouri, 1987, J. Chem. Phys. **87**, 1892.
Hirst, D. M., 1985, *Potential Energy Surfaces* (Taylor and Francis, London).
Howard, R. E., A. D. McLean, and W. A. Lester, Jr., 1979, J. Chem. Phys. **71**, 2412.
Hoy, A. R., I. M. Mills, and G. Strey, 1972, Mol. Phys. **24**, 1265.
Jacobson, K. N., J. K. Norskov, and M. J. Puska, 1987, Phys. Rev. B **35**, 7423.
Jacox, M., 1987, J. Chem. Phys. **87**, 5809.
Jasien, P. G., and R. Shepard, 1988, Int. J. Quantum Chem. Symp. **S22**, 183.
Johnson, B. R., and N. W. Winter, 1977, J. Chem. Phys. **66**, 4116.
Johnston, H. S., 1966, *Gas Phase Reaction Rate Theory* (Ronald, New York).
Johnston, H. S., and C. A. Parr, 1963, J. Am. Chem. Soc. **85**, 2544.
Joseph, T., R. Steckler, and D. G. Truhlar, 1987, J. Chem. Phys. **87**, 7036.
Joseph. T., D. G. Truhlar, and B. C. Garrett, 1988, J. Chem. Phys. **88**, 6982.
Kollman, P., 1987, Annu. Rev. Phys. Chem. **38**, 303.
Krenos, J. R., K. K. Lehmann, J. C. Tully, P. M. Hierl, and G. P. Smith, 1976, Chem. Phys. **16**, 109.
Kress, J. D., and A. E. DePristo, 1988, J. Chem. Phys. **88**, 2596.
Kuntz, P. J., 1976, in *Dynamics of Molecular Collisions, Part B,* edited by W. H. Miller (Plenum, New York), Chap. 2.
Kuntz, P. J., 1979, in *Atom-Molecule Collision Theory,* edited by

R. B. Bernstein (Plenum, New York), p. 79.
Kuntz, P. J., 1985, in *Theory of Chemical Reaction Dynamics,* edited by M. Baer (CRC Press, Boca Raton, FL), p. 71.
Kuntz, P. J., E. M. Nemeth, J. C. Polanyi, S. D. Rosner, and C. E. Young, 1966, J. Chem. Phys. **44**, 1168.
Kuntz, P. J., B. I. Niefer, and J. J. Sloan, 1988, J. Chem. Phys. **88**, 3629.
Last, I., and M. Baer, 1981, J. Chem. Phys. **75**, 288.
Last, I., and M. Baer, 1986, Int. J. Quantum Chem. **29**, 1067.
Last, I., and M. Baer, 1987, J. Chem. Phys. **86**, 5534.
Lee, K. T., J. M. Bowman, A. F. Wagner, and G. C. Schatz, 1982, J. Chem. Phys. **76**, 3563 (Part II), 3583 (Part III).
Liu, B. J., 1973, Chem. Phys. **58**, 1925.
Loesch, H., 1987, Chem. Phys. **112**, 85.
Marcus, R. A., 1966, J. Chem. Phys. **45**, 4493.
McLauglin, D. R., and D. L. Thompson, 1973, Chem. Phys. **59**, 4393.
Melius, C. F., and R. Blint, 1979, J. Chem. Phys. Lett. **64**, 183.
Michael, J. V., 1989, J. Chem. Phys. **90**, 189.
Miller, W. H., N. C. Handy, and J. E. Adams, 1980, J. Chem. Phys. **72**, 99.
Murrell, J. N., and S. Carter, 1984, J. Phys. Chem. **88**, 4887.
Murrell, J. N., S. Carter, S. C. Farantos, P. Huxley, and A. J. C. Varandas, 1984, *Molecular Potential Energy Functions* (Wiley, New York).
Murrell, J. N., S. Carter, I. M. Mills, and M. F. Guest, 1981, Mol. Phys. **42**, 605.
Murrell, J. N., and J. A. Rodriguez, 1986, J. Mol. Struct. (Theochem.) **139**, 267.
Pederson, L., and R. N. Porter, 1967, J. Chem. Phys. **47**, 4751.
Persky, A., and H. Kornweitz, 1987, J. Phys. Chem. **91**, 5496.
Polak, R., 1976, Chem. Phys. **16**, 353.
Pollak, E., M. Baer, N. Abu-Salbi, and D. J. Kouri, 1985, J. Chem. Phys. **99**, 15.
Presser, N., and R. J. Gordon, 1985, J. Chem. Phys. **82**, 1291.
Raff, L. M., 1987, J. Phys. Chem. **91**, 3266.
Redmon, M. J., and G. C. Schatz, 1981, Chem. Phys. **54**, 365.
Reimers, J. R., and R. O. Watts, 1984, Chem. Phys. **85**, 83.
Robie, D. C., S. Arepalli, N. Presser, T. Kitsopoulos, and R. Gordon, 1987, J. Chem. Phys. Lett. **134**, 579.
Sathyamurthy, N., 1985, Comput. Phys. Rep. **3**, 1.
Sathyamurthy, N., and L. M. Raff, 1975, J. Chem. Phys. **63**, 464.
Sathyamurthy, N., R. Rangarajan, and L. M. Raff, 1976, J. Chem. Phys. **64**, 4606.
Sato, S., 1955a, J. Chem. Phys. **23**, 592.
Sato, S., 1955b, Bull. Chem. Soc. Jpn. **28**, 450.
Sato, S., 1955c, J. Chem. Phys. **23**, 2465.
Schatz, G. C., 1981, in *Potential Energy Surfaces and Dynamics Calculations,* edited by D. G. Truhlar (Plenum, New York), p. 287.
Schatz, G. C., 1985, J. Chem. Phys. **83**, 5677.
Schatz, G. C., 1988a, Chem. Phys. Lett. **150**, 92.
Schatz, G. C., 1988b, Annu. Rev. Phys. Chem. **39**, 317.
Schatz, G. C., B. Amaee, and J. N. L. Connor, 1987, Comput. Phys. Commun. **47**, 45.
Schatz, G. C., B. Amaee, and J. N. L. Connor, 1988, J. Phys. Chem. **92**, 3190.
Schatz, G. C., M. S. Fitzcharles, and L. B. Harding, 1987, Faraday Discuss. Chem. Soc. **84**, 359.
Schatz, G. C., A. F. Wagner, S. P. Walch, and J. M. Bowman, 1981, J. Chem. Phys. **74**, 4984.
Schinke, R., 1984, J. Chem. Phys. **80**, 5510.
Schinke, R., and W. A. Lester, Jr., 1979, J. Chem. Phys. **70**, 4893.
Schinke, R., and W. A. Lester, Jr., 1980, J. Chem. Phys. **72**, 3754.
Siegbahn, P., and B. Liu, 1978, J. Chem. Phys. **68**, 2457.
Simons, G., 1974, J. Chem. Phys. **61**, 369.
Simons, G., R. G. Parr, and J. M. Finlan, 1973, J. Chem. Phys. **59**, 3229.
Smith, I. W. M., 1975, J. Chem. Soc. Faraday Trans. 2 **71**, 1970.
Smith, I. W. M., and P. Wood, 1973, Mol. Phys. **25**, 441.
Sorbie, K. S., and J N. Murrell, 1976, Mol. Phys. **29**, 1387.
Steckler, R., K. J. Dykema, F. B. Brown, G. C. Hancock, D. G. Truhlar, and T. Valencich, 1987, J. Chem. Phys. **87**, 7024.
Steckler, R., D. G. Truhlar, and B. C. Garrett, 1985, J. Chem. Phys. **83**, 2870.
Stine, J. R., and J. T. Muckerman, 1976, J. Chem. Phys. **65**, 3975.
Stine, J. R., and J. T. Muckerman, 1978, J. Chem. Phys. **68**, 185.
Stone, A. J., and S. C. Price, 1988, J. Phys. Chem. **92**, 3325.
Sumpter, B. G., and D. L. Thompson, 1987, J. Chem. Phys. **87**, 5809.
Takayanagi, T., and S. Sato, 1988, Chem. Phys. Lett. **144**, 191.
Thommarson, R. L., and G. C. Berend, 1973, Int. J. Chem. Kinet. **5**, 629.
Thompson, D. L., 1972, J. Chem. Phys. **56**, 3570.
Truhlar, D. G., and C. J. Horowitz, 1978, J. Chem. Phys. **68**, 2466; **71**, 1514(E).
Truhlar, D. G., K. Runge, and B. C. Garrett, 1984, in *Proceedings of the Twentieth International Symposium on Combustion* (Combustion Institute, Pittsburgh), p. 585.
Truhlar, D. G., R. Steckler, and M. S. Gordon, 1987, Chem. Rev. **87**, 217.
Tully, J. C., 1977, in *Semi-Empirical Methods of Electronic Structure Calculation, Part A: Techniques,* edited by G. D. Segal (Plenum, New York), Chap. 6.
Varandas, A. J. C., F. B. Brown, C. A. Mead, D. G. Truhlar, and N. C. Blais, 1987, J. Chem. Phys. **86**, 6258.
Viswanathan, R., D. L. Thompson, and L. M. Raff, 1985, J. Phys. Chem. **89**, 1428.
Wadt, W. R., and N. Winter, 1977, J. Chem. Phys. **67**, 3069.
Wagner, A. F., and J. M. Bowman, 1987, J. Chem. Phys. **86**, 1976.
Wagner, A. F., G. C. Schatz, and J. M. Bowman, 1981, J. Chem. Phys. **74**, 4960.
Walch, S. P., 1987, J. Chem. Phys. **86**, 5670.
Walch, S.. P., and L. B. Harding, 1988, J. Chem. Phys. **88**, 7653.
Westenberg, A. A., and N. de Haas, 1967, J. Chem. Phys. **47**, 4241.
White, K. A., and G. C. Schatz, 1984, J. Phys. Chem. **88**, 2049.
Whitlock, P. A., J. T. Muckerman, and E. R. Fisher, 1976, *Theoretical Investigations of the Energetics and Dynamics of the Reactions* $O(^3P,^1D)+H_2$ *and* $C(^1D)+H_2$ (Research Institute for Engineering Sciences, Wayne State University, Detroit).
Whitlock, P. A., J. T. Muckerman, and E. R. Fisher, 1982, J. Chem. Phys. **76**, 4468.
Wight, C. A., and S. R. Leone, 1983a, J. Chem. Phys. **78**, 4875
Wight, C. A., and S. R. Leone, 1983b, J. Chem. Phys. **79**, 4823.
Wilkins, R. L., 1975, J. Chem. Phys. **63**, 534.
Witriol, N. M., J. D. Stettler, M. A. Ratner, J. R. Sabin, and S. Trickey, 1977, J. Chem. Phys. **66**, 1141.
Wright, J. S., and S. K. Gray, 1978, J. Chem. Phys. **69**, 67.
Zhu, Y-F., S. Arepalli, and R. J. Gordon, 1989, J. Chem. Phys. **90**, 183.